HHS Public Access

Author manuscript

J Comp Neurol. Author manuscript; available in PMC 2018 May 22.

Published in final edited form as:

J Comp Neurol. 2017 August 01; 525(11): 2592–2610. doi:10.1002/cne.24226.

Seizure frequency correlates with loss of dentate gyrus GABAergic neurons in a mouse model of temporal lobe epilepsy

Paul S. Buckmaster[1,2], **Emily Abrams**[1], and **Xiling Wen**[1]

[1]Department of Comparative Medicine, Stanford University, Stanford, California

[2]Department of Neurology & Neurological Sciences, Stanford University, Stanford, California

Abstract

Epilepsy occurs in one of 26 people. Temporal lobe epilepsy is common and can be difficult to treat effectively. It can develop after brain injuries that damage the hippocampus. Multiple pathophysiological mechanisms involving the hippocampal dentate gyrus have been proposed. This study evaluated a mouse model of temporal lobe epilepsy to test which pathological changes in the dentate gyrus correlate with seizure frequency and help prioritize potential mechanisms for further study. FVB mice (n = 127) that had experienced status epilepticus after systemic treatment with pilocarpine 31–61 days earlier were video-monitored for spontaneous, convulsive seizures 9 hr/day every day for 24–36 days. Over 4,060 seizures were observed. Seizure frequency ranged from an average of one every 3.6 days to one every 2.1 hr. Hippocampal sections were processed for Nissl stain, Prox1-immunocytochemistry, GluR2-immunocytochemistry, Timm stain, glial fibrillary acidic protein-immunocytochemistry, glutamic acid decarboxylase in situ hybridization, and parvalbumin-immunocytochemistry. Stereological methods were used to measure hilar ectopic granule cells, mossy cells, mossy fiber sprouting, astrogliosis, and GABAergic interneurons. Seizure frequency was not significantly correlated with the generation of hilar ectopic granule cells, the number of mossy cells, the extent of mossy fiber sprouting, the extent of astrogliosis, or the number of GABAergic interneurons in the molecular layer or hilus. Seizure frequency significantly correlated with the loss of GABAergic interneurons in or adjacent to the granule cell layer, but not with the loss of parvalbumin-positive interneurons. These findings prioritize the loss of granule cell layer interneurons for further testing as a potential cause of temporal lobe epilepsy.

Keywords

GFAP; hippocampus; mossy cell; pilocarpine; Prox1; Timm stain; RRID: AB_10064230; RRID: AB_10000344; RRID: AB_2247874; RRID: AB_10013382

Correspondence: Paul S. Buckmaster, Department of Comparative Medicine, Stanford University, 300 Pasteur Drive, R321 Edwards Building, Stanford, CA 94305. psb@stanford.edu.

CONFLICT OF INTEREST STATEMENT

The authors have no conflicts of interest.

ROLE OF AUTHORS

All authors had full access to all the data in the study and take responsibility for the integrity of the data and the accuracy of the data analysis. Study concept and design, drafting of manuscript, statistical analysis, obtained funding, study supervision: PSB. Acquisition of data: EA, XW, PSB. Analysis and interpretation of data: EA, XW, PSB.

1 INTRODUCTION

In patients with temporal lobe epilepsy, seizures usually start in the hippocampus (Quesney, 1986; Spanedda, Cendes, & Gotman, 1997; Spencer, Williamson, Spencer, & Mattson, 1987; Sperling & O'Connor, 1989). The hippocampal dentate gyrus has been suspected to play a role in seizure initiation. In patients, the dentate gyrus is hyperexcitable (Franck, Pokorny, Kunkel, & Schwartzkroin, 1995; Gabriel et al., 2004; Masukawa, Wang, O'Connor, & Uruno, 1996). It displays pathological abnormalities, including loss of some hilar mossy cells (Blümcke et al., 1999; Margerison & Corsellis, 1966), but not all (Seress et al., 2009), fewer inhibitory interneurons (Babb, Pretorius, Kupfer, & Crandall, 1989; de Lanerolle, Kim, Robbins, & Spencer, 1989; Mathern, Babb, Pretorius, & Leite, 1995), synaptic reorganization of granule cells (Babb, Kupfer, Pretorius, Crandall, & Levesque, 1991; Houser et al., 1990; Sutula, Cascino, Cavazos, Parada, & Ramirez, 1989), generation of hilar ectopic granule cells (Houser, 1990; Parent, Elliott, Pleasure, Barbaro, & Lowenstein, 2006), and astrogliosis (Das et al., 2012; Johnson et al., 2016; Van Paesschen, Revesz, Duncan, King, & Connelly, 1997).

Each pathological abnormality listed above could be an epileptogenic mechanism. Loss of GABAergic interneurons would directly reduce inhibition of granule cells, the major excitatory neuron type of the dentate gyrus. Loss of mossy cells has been proposed to indirectly reduce inhibition of granule cells (Sloviter, 1987, 1994; Sloviter et al., 2003). In contrast, surviving mossy cells have been proposed to be pro-epileptic by amplifying excessive activity of granule cells (Ratzliff, Santhakumar, Howard, & Soltesz, 2002; Santhakumar et al., 2000) and by bridging hyperactivity from burst-firing CA3 pyramidal cells to granule cells (Scharfman, Smith, Goodman, & Sollas, 2001). Granule cell axon (mossy fiber) sprouting has been proposed to cause seizures by increasing recurrent excitation (Tauck & Nadler, 1985) and by indirectly reducing inhibition (Buhl, Otis, & Mody, 1996). Hilar ectopic granule cells have been proposed to be burst-firing super-connected hubs that can trigger seizures (Cameron, Zhan, & Nadler, 2011; Scharfman & Pierce, 2012). Astrogliosis has been proposed to be epileptogenic by multiple mechanisms (Binder & Steinhäuser, 2006; Gibbons, Smeal, Takahashi, Vargas, & Wilcox, 2013; Wetherington, Serrano, & Dingledine, 2008), including loss of cell domain organization (Oberheim et al., 2008), inflammation (Maroso et al., 2010), reduced inhibition (Ortinski et al., 2010), glutamate release (Clasadonte, Dong, Hines, & Haydon, 2013), disruption of adenosine homeostasis (Boison, 2016), and altered expression of chloride ion pumps (Robel & Sontheimer, 2016).

It is unclear if any of the pathological abnormalities in the dentate gyrus are epileptogenic. If a pathological abnormality were epileptogenic, then its severity might correlate with the frequency of spontaneous seizures. The underlying (and arguable) assumption is that if an abnormality causes seizures, then more of the abnormality would cause more seizures. If so, multiple mechanisms could be evaluated together in a single group of experimental subjects, revealing their relative importance. Hester and Danzer (2013) used this approach. They reported that the percentage of hilar ectopic granule cells, the amount of mossy fiber sprouting, and the extent of mossy cell loss all correlated with seizure frequency. The study,

however, had limitations. Only nine epileptic mice were included, modern stereological methods were not used, and inhibitory interneurons were not evaluated.

In this study, seizure frequency and pathological abnormalities of the dentate gyrus were measured in an animal model of temporal lobe epilepsy. Pathological abnormalities were quantified using unbiased stereological techniques and tested for correlation with seizure frequency in 127 epileptic pilocarpine-treated mice. Hilar ectopic granule cells were labeled by Prospero homeobox 1 (Prox1)-immunocytochemistry, mossy cells were identified by GluR2-immunocytochemistry, mossy fiber sprouting was visualized with the Timm stain, astrogliosis was assessed by glial fibrillary acidic protein (GFAP)-immunocytochemistry, and GABAergic interneurons were labeled by in situ hybridization for glutamic acid decarboxylase (GAD) and immunocytochemistry for parvalbumin. We asked, which pathological abnormalities of the dentate gyrus correlate with seizure frequency?

2 MATERIALS AND METHODS

2.1 Animals

All experiments were performed in accordance with the National Institutes of Health *Guide for the Care and Use of Laboratory Animals* and approved by an institutional animal care and use committee at Stanford University. Mice were housed in micro-isolator cages on wood shavings in groups of up to five. Cotton nestlets were provided for enrichment. Room lights were on from 7:00 a.m. till 7:00 p.m. Mice had unlimited access to rodent chow and water. Female (n = 83) and male (n = 45) GIN mice (FVBTg(GadGFP)45704Swn/J, The Jackson Laboratory, RRID:IMSR_JAX:003718) were treated with pilocarpine (300 mg/kg, i.p.) ~45 min after atropine methylbromide (5 mg/kg, i.p.) when they were 58 ± 2 days old (mean ± *SEM*, range, 28–129 days). Diazepam (10 mg/kg, i.p.) was administered 2 hr after the onset of stage 3 or greater seizures (Racine, 1972), and repeated as needed to suppress convulsions. During recovery, mice were kept warm with a heating pad and received lactated Ringer's with dextrose subcutaneously. Naïve control mice (n = 3 females, 7 males) did not undergo pilocarpine treatment.

2.2 Seizure monitoring

Beginning 42 ± 1 days (range, 31–61 days) after pilocarpine treatment, mice were video-recorded, beginning at approximately 8:00 a.m., for 9 hr/day every day for 29 ± 0.2 days (range, 24–36 days). For recording, mice were moved to the laboratory and transferred from their home cage to an aquarium divided into 10 slots. Each slot contained one mouse. Recordings of 10 mice at a time were manually reviewed in the fast-forward playback setting for behavioral seizures of grade 3 (fore-limb clonus) or greater. Seizure frequency was measured by an investigator who was blind to the anatomical results of this study.

After seizure monitoring was complete, mice were killed by urethane overdose (2 g/kg i.p.). Mice were perfused immediately through the ascending aorta at 15 ml/min for 2 min with 0.9% sodium chloride, 5 min with 0.37% sodium sulfide, 1 min with 0.9% sodium chloride, and 30 min with 4% formaldehyde in 0.1 M phosphate buffer (PB, pH 7.4). Epileptic pilocarpine-treated mice were 129 ± 2 days old (range, 91–197 days) when they were

perfused. Controls were 110 ± 21 days old (range, 41–198 days). Brains were post-fixed overnight at 4°C. The right hippocampus was isolated, equilibrated in 30% sucrose in PB, frozen, and stored at −80°C. Hippocampi were thawed in 30% sucrose in PB, gently straightened, frozen, and sectioned transversely from the septal pole to the temporal pole with a microtome set at 40 μm. Sections were collected in 30% ethylene glycol and 25% glycerol in 50 mM PB and stored at −20°C.

2.3 Section sampling

In patients with temporal lobe epilepsy, pathology can vary along the septotemporal length of the hippocampus (Babb et al., 1984; Dam, 1980; Masukawa et al., 1995; Thom et al., 2012). Therefore, starting at a random point near the septal pole, series of sections from the entire septotemporal length of the hippocampus were sampled. A 1-in-12 series yielded an average of 15 sections/hippocampus. A 1-in-12 series of sections was processed for Nissl stain with 0.25% thionin. Section sampling parameters for other stains are listed in Table 1. For the Timm stain, three sections per hippocampus were analyzed: one section from the middle of the most septal third of the hippocampus (17% of the distance from the septal pole to the temporal pole), one from the middle of the middle third of the hippocampus (50%), and one from the middle of the temporal third (84%).

2.4 Staining

For Timm staining, sections were mounted on gelatin-coated slides and dried overnight. Timm staining developed at room temperature in the dark for 45 min in 120 ml 50% gum arabic, 20 ml 2 M citrate buffer, 60 ml 0.5 M hydroquinone, and 1 ml 19% silver nitrate. After rinsing in water, sections were exposed to 5% sodium thiosulfate for 4 min before dehydration and coverslipping with distyrene plasticizer xylene (DPX).

For immunocytochemistry, free-floating sections were rinsed in PB and treated with 1% H_2O_2 for 2 hr. After rinses in PB and 0.1 M tris-buffered saline (TBS, pH 7.4), sections were treated with blocking solution consisting of 3% goat serum, 2% bovine serum albumin (BSA), and 0.3% Triton X-100 in 0.05 M TBS for 2 hr. Sections were rinsed in TBS and incubated for 7 days at 4°C in primary antibody (Table 2) diluted in 1% goat serum, 0.2% BSA, and 0.3% Triton X-100 in 0.05 M TBS. After rinses in TBS, sections incubated for 2 hr in biotinylated goat anti-rabbit serum (1 : 500, Vector Laboratories, Burlingame, CA) in secondary diluent consisting of 2% BSA and 0.3% Triton X-100 in 0.05 M TBS. After rinses in TBS, sections incubated for 2 hr in avidin-biotin-horseradish peroxidase complex (1 : 500, Vector Laboratories) in secondary diluent. After rinses in TBS and 0.1 M tris buffer (TB, pH 7.6), sections were placed for 5 min in chromogen solution consisting of 0.02% diaminobenzidine, 0.04% NH_4Cl, and 0.015% glucose oxidase in TB and then transferred to fresh chromogen solution with 0.1% β-D-glucose until cell staining reached desired levels, which typically required 13 min. The reaction was stopped in rinses of TB. Sections were mounted and dried on gelatin-coated slides, dehydrated, cleared, and coverslipped with DPX.

Another series of sections was processed for in situ hybridization for GAD. GAD65-cDNA (kindly provided by Drs. A. Tobin and N. Tillakaratne, University of California at Los

Angeles) was ~2.3 kb, isolated from a λ ZapII library from adult rat hippocampus (Erlander, Tillakaratne, Feldblum, Patel, & Tobin, 1991). GAD65-cDNA included the entire coding region (~1755 bp), ~74 bp of the 5′ untranslated region, and ~467 bp of the 3′ untranslated region (Dr. N. Tillakaratne, University of California at Los Angeles, personal communication). RNA probes were produced by transcription of GAD65-cDNA, using a nonradioactive RNA labeling kit (Roche, Basel, Switzerland). Sections were washed in 10 mM phosphate buffered saline (PBS) and incubated sequentially in 0.02 N HCl, 0.01% Triton X-100 in PBS, 0.2 μg/ml proteinase K in 50 mM tris (pH 7.4), 5 mM EDTA, and 2 mg/ml glycine in PBS. Sections prehybridized for 1 hr in a solution containing 50% formamide, 750 mM NaCl, 25 mM EDTA, 25 mM piperazine-*N,N*′-bis 2-ethanesulfonic acid, 0.2% sodium dodecyl sulfate, 250 μg/ml poly A, and 250 μg/ml salmon sperm DNA. Sections hybridized overnight in a humid chamber at 50°C in a solution consisting of the prehybridization solution with digoxygenin-labeled RNA probe at a concentration of 2–4 μl/ml, 100 mM dithiothreitol, 4% dextran sulfate, and 250 μg/ml tRNA. After hybridization, sections were subjected to RNase treatment and stringency washes. Sections were processed for immunodetection of digoxygenin label with reagents of a nonradioactive nucleic acid detection kit (Roche), mounted on gelatin-coated slides, and coverslipped with ImmunoHistoMount (Sigma, St. Louis, MO) and DPX.

2.5 Antibody characterization

Primary antibodies are described in Table 2. Granule cells express Prox1 (Liu et al., 2000). Polyclonal anti-Prox1 serum (Covance, Princeton, NJ) (RRID: AB_10064230) was used to label ectopic granule cells. Specificity of the antibody is supported by reduced labeling in conditional Prox1 knockout mice (Lavado, Lagutin, Chow, Baker, & Oliver, 2010). The antibody stained a pattern consistent with hilar ectopic granule cells demonstrated previously with different antibodies (Jiao & Nadler, 2007; McCloskey, Hintz, Pierce, & Scharfman, 2006).

Parvalbumin antibody (Swant, Marly, Switzerland) (RRID: AB_10000344) was used to label a subtype of GABAergic interneuron. According to the manufacturer's data sheet, the antibody did not stain cells in the brain of parvalbumin knockout mice. In the mouse hippocampus, the antibody stained a pattern consistent with parvalbumin-positive neurons demonstrated previously (Kosaka, Katsumaru, Hama, Wu, & Heizmann, 1987).

Mossy cells can be distinguished from GABAergic interneurons in the hilus by expression of GluR2 (Leranth, Szeidemann, Hsu, & Buzsáki, 1996). GluR2 antibody (Millipore, Temecula, CA) (RRID: AB_2247874) was used to label mossy cells. According to the manufacturer's data sheet, Western blot analysis of transfected cells is selective for GluR2 with no cross reaction with GluR1, GluR3, or GlurR4. A single band of 108 kDa is detected in Western blots of rat brain. In the mouse dentate gyrus, the GluR2 antibody stained a pattern consistent with mossy cells, as demonstrated previously (Fujise, Liu, Hori, & Kosaka, 1998).

GFAP antibody (Dako, Glostrup, Denmark) (RRID: AB_10013382) was used to label astrocytes. According to the manufacturer's data sheet, the antibody is solid-phase absorbed with human and cow serum proteins. It shows one distinct precipitate (GFAP) with cow

brain extract. And it shows no reaction with human plasma or cow serum. In the mouse hippocampus, it stained a pattern consistent with fibrillary astrocytes, as demonstrated previously with a different antibody (Hubbard, Szu, Yonan, & Binder, 2016). Evidence for specificity of this antibody includes lack of staining in GFAP knockout mice (Hanbury, Ling, Wuu, & Kordower, 2003).

2.6 Analysis

All anatomical analyses were performed by investigators who were blind to seizure frequency results. A Neurolucida system (MBF Bio-sciences, Williston, VT) was used to count neuron profiles. Mossy cells were identified as large (>12 μm soma diameter) GluR2-positive cell body profiles in the hilus. The hilus was defined by its border with the granule cell layer and by straight lines from the ends of the granule cell layer to the proximal tip of the CA3 pyramidal cell layer. Hilar ectopic granule cells were identified as Prox1-positive cell body profiles in the hilus that were displaced at least 25 μm from the granule cell layer. GAD- and parvalbumin-positive cell body profiles were counted any-where in the dentate gyrus. GAD-positive cell body position was specified as either being in or touching the granule cell layer, in the molecular layer, or in the hilus. Counts of neuron profiles were used to estimate the number of neurons per hippocampus, as described in the Results section.

Mossy fiber sprouting was measured as the percentage of the granule cell layer plus molecular layer that was black after Timm staining. For all sections, an image of the dentate gyrus was obtained with a 10× objective using identical microscope and camera settings. NIH ImageJ was used to measure the area of a contour drawn around the granule cell layer plus molecular layer. The Timm-positive area within the contour was selected by adjusting a darkness threshold until all of the black area was covered. The average percent area that was Timm-positive for the three sections of each mouse was calculated.

Astrogliosis was measured as the percentage of the dentate gyrus area that was GFAP-positive. For GFAP-immunocytochemistry, all sections from all animals were processed together in the same solutions and for the same durations. An image of the dentate gyrus was obtained from each section with a 10× objective using identical microscope and camera settings. NIH ImageJ was used to measure the area of a contour drawn around the dentate gyrus (molecular layer, granule cell layer, and hilus). The GFAP-positive area within the contour was determined by setting a darkness threshold to a constant setting. The darkness threshold was determined in a pilot study of control animal sections. The average threshold setting that optimally detected astrocytes and their processes in control animals was 165. That threshold setting was used to measure the GFAP-positive area in all of the sections from all of the animals. An average value from all of the sections of each animal was calculated.

2.7 Statistics

SigmaPlot 12 (Systat, San Jose, CA) was used for statistical analyses. Results are reported as mean ± *SEM*. Differences were considered significant if $p < 0.05$. Two-tailed *t* tests were used. The Shapiro-Wilk test or Kolmogorov-Smirnov test with Lilliefors correction was used to measure normality. Equal variance was tested by checking the variability about the group

means. If normality or equal variance tests failed, a Mann–Whitney rank sum test was used. Linear regression was used to measure the strength of the association between pairs of variables. If residuals were not normally distributed with constant variance, data were log-transformed. If residuals still were not normally distributed with constant variance, the Spearman rank order correlation was performed.

2.8 Images

Photoshop (Adobe, San Jose, CA) was used to process images. Only brightness and contrast were adjusted.

3 RESULTS

3.1 Epileptic pilocarpine-treated mice display a range of seizure frequencies

Over 29,850 mouse-hours of video were analyzed. The seizure monitoring period began 31–61 days after status epilepticus. All of the mice that had experienced status epilepticus after pilocarpine treatment displayed spontaneous behavioral seizures that involved forelimb clonus. A total of 4,063 seizures were observed. Seizure frequency data obtained from a group of 10 pilocarpine-treated mice is shown in Figure 1a. Seizure clusters were evident in some of the mice, as reported previously (Mazzuferi, Kumar, Rospo, & Kaminski, 2012). The mean and median seizure frequencies were 0.132 and 0.111 seizures/h, respectively (Figure 1b). There was a substantial range in seizure frequency: 0.012–0.473 seizures/h, which is an average of one seizure every 3.6 days–2.1 hr. The standard deviation was 0.084 seizures/h. The coefficient of variation was 0.636.

One female mouse was omitted from analysis. She required early euthanasia, because of morbidity after experiencing many recurrent seizures (>37 during one recording period). Her average seizure frequency was 10 standard deviations higher than the group average. It has been reported that some female FVB mice, usually >16 weeks of age, develop spontaneous seizures that can be fatal (Goelz et al., 1998; Mahler, Stokes, Mann, Takaoka, & Maronpot, 1996; Rosenbaum, VandeWoude, & Bielefeldt-Ohmann, 2007). The underlying epileptogenic mechanism in older female FVB mice is unclear. In this study, seizure frequency was not significantly different in female (0.120 ± 0.007 seizures/h) and male mice (0.152 ± 0.016 seizures/h, $p = 0.327$, Mann–Whitney rank sum test) (Figure 1c).

3.2 No significant effect of obvious pyramidal cell loss on seizure frequency

Nissl stained sections were screened qualitatively for obvious neuron loss in the hippocampus. Compared to controls (Figure 2a1), 100% (124/124) of the epileptic mice displayed obvious hilar neuron loss (Figure 2a2). Most of the epileptic mice (83/124, 67%) displayed no other obvious neuron loss, except hilar neuron loss (Figure 2b). In some epileptic mice, pyramidal cell loss was evident in CA1 (2/124, 2%), CA3 (17/124, 14%), or both CA1 and CA3 (22/124, 18%) (Figure 2a3). Seizure frequency was not significantly different in mice without obvious loss of pyramidal cells (0.127 ± 0.009 seizures/h) and mice with obvious loss of pyramidal cells (0.141 ± 0.014 seizures/h, $p = 0.426$, Mann–Whitney rank sum test) (Figure 2c). This qualitative analysis does not exclude the possibility of more subtle neuron loss in cornu ammonis contributing to epileptogenesis. However,

these findings are consistent with this study's focus on the dentate gyrus for testing pathological abnormalities correlated with seizure frequency.

Previously, we used a similar pilocarpine-treatment protocol to generate epileptic mice of the background strain C57BL/6J (Hofmann, Balgooyen, Mattis, Deisseroth, & Buckmaster, 2016). In epileptic C57BL/6J mice, 86% (25/29) display obvious loss of pyramidal cells, which is significantly more than the FVB mice of this study (18%, 41/124, p <0.001, chi-squared test). These findings provide additional evidence for differences in the severity of hippocampal pathology in mouse models of temporal lobe epilepsy based on different background strains.

3.3 No significant correlation between the number of hilar ectopic granule cells and seizure frequency

In control mice, Prox1-positive neurons were abundant in the granule cell layer (Figure 3a1). Hilar ectopic granule cells were identified as Prox1-positive neurons in the hilus, located at least 25 μm away from the granule cell layer. Hilar ectopic Prox1-positive neurons were present in control mice, but rare. There were more hilar ectopic Prox1-positive profiles per section in the temporal part of the hippocampus (Figure 3c).

In epileptic mice, the dentate gyrus appeared hypertrophied (Figure 3a2). There appeared to be more Prox1-positive neurons in the granule cell layer and in the hilus at all septotemporal levels of the hippocampus (Figure 3c). Previous studies have shown that in mouse models of temporal lobe epilepsy (Bouilleret et al., 1999), including pilocarpine-treated mice (Heng, Haney, & Buckmaster, 2013; Lew & Buckmaster, 2011; Zhang et al., 2009), the dentate gyrus is larger and contains more granule cells, compared to controls (Buckmaster & Lew, 2011).

In a subset of mice, a Stereo Investigator system (MBF Biosciences) and the optical fractionator method (West, Slomianka, & Gundersen, 1991) were used to estimate the total number of hilar Prox1-positive neurons per dentate gyrus. Parameters of the optical fractionator method are listed in Table 1. There was a high correlation (R = 0.998) between the number of profiles counted and the total number of neurons estimated by the optical fractionator method (Figure 3b). The slope of the regression line was used to estimate the total number of hilar ectopic Prox1-positive neurons per dentate gyrus from the profile counts for all of the mice. The mean number of hilar ectopic Prox1-positive neurons per dentate gyrus in epileptic mice (2190 ± 80) was 3.7× greater than that of controls (600 ± 30, p <0.001, Mann–Whitney rank sum test) (Figure 3d). There was no significant correlation between the number of hilar ectopic Prox1-positive neurons and seizure frequency (R = 0.0763, p = 0.398, ANOVA) (Figure 3e).

3.4 No significant correlation between the number of mossy cells and seizure frequency

In control mice, GluR2-positive neurons were abundant in the granule cell layer, pyramidal cell layer, and hilus (Figure 4a1). Large GluR2-positive neurons in the hilus were considered to be mossy cells, as in previous studies (Fujise & Kosaka, 1999). GluR2-positive soma profiles in the hilus were counted if their diameter was >12 μm. They were more abundant in sections from the temporal end of the hippocampus (Figure 4c).

In epileptic mice, the hilus appeared to contain fewer large GluR2-positive neurons (Figure 4a2), as reported previously (Tang et al., 2005; Zhang, Thamattoor, LeRoy, & Buckmaster, 2015). More small GluR2-positive neurons (<12 μm soma diameter) were evident, but they were likely to be ectopic granule cells (Jiao & Nadler, 2007). The number of large, hilar GluR2-positive neuron profiles was reduced in epileptic mice at all septotemporal levels of the hippocampus (Figure 4c).

There was a high correlation ($R = 0.997$) between the number of large, hilar GluR2-positive profiles counted and the total number of large, hilar GluR2-positive neurons per dentate gyrus estimated by the optical fractionator method in a subset of mice (Figure 4b, Table 1). The slope of the regression line was used to estimate the number of large, hilar GluR2-positive neurons per dentate gyrus from the profile counts for all of the mice. The mean number per dentate gyrus in epileptic mice (1270 ± 60) was only 38% of that in controls (3300 ± 250, $p < 0.001$, Mann–Whitney rank sum test) (Figure 4d). There was no significant correlation between the number of large, hilar GluR2-positive neurons and seizure frequency ($R = 0.156$, $p = 0.079$, ANOVA) (Figure 4e).

3.5 No significant correlation between the extent of mossy fiber sprouting and seizure frequency

In the dentate gyrus of control mice, black Timm staining was almost entirely restricted to the hilus (Figure 5a1). In all of the epileptic pilocarpine-treated mice, black Timm staining was also evident in the granule cell layer and molecular layer (Figure 5a2), which indicates mossy fiber sprouting (Nadler, Perry, & Cotman, 1980).

In previous studies, we measured the percent area of the granule cell layer plus molecular layer labeled with black Timm staining in 1-in-12 series of sections from the entire septotemporal length of the hippocampus (Buckmaster & Lew, 2011; Heng et al., 2013; Lew & Buckmaster, 2011). Those data were re-analyzed to test whether sampling fewer sections/mouse would provide results similar to those derived from the entire sample. The following section sampling schemes were tested: one section from the middle of the hippocampus (50% of the distance from the septal pole to the temporal pole), 17, 33, 67, or 84%; the average of three sections from 33, 50, and 67%; and the average of three sections from 17, 50, and 84%. Data from each section sampling scheme were plotted against results from the entire 1-in-12 series. The highest correlation coefficient was obtained from averaging three sections from 17, 50, and 84%. Figure 5b shows the plot of that sampling scheme versus the entire 1-in-12 series (slope = 1.049, $R = 0.961$, $p < 0.001$, Spearman rank order correlation). Therefore, in this study, mossy fiber sprouting was quantified as the average percent area of black Timm staining in the granule cell layer plus molecular layer of sections from the middle of the septal (17%), middle (50%), and temporal (84%) thirds of the hippocampus.

The average percent area of black Timm staining in epileptic mice (22.5 ± 0.3%) was 12.5× greater than in controls (1.8 ± 0.5%, $p \leq 0.001$, Mann–Whitney rank sum test) (Figure 5d). Epileptic mice had substantially larger percent areas of black Timm staining at all three levels analyzed, especially the temporal level (Figure 5c). There was a significant negative correlation between the percent area of black Timm staining and the number of large, hilar GluR2-positive neurons per dentate gyrus ($R = 0.515$, $p < 0.001$, ANOVA) (Figure 5e). This

finding revealed an association of mossy cell loss with mossy fiber sprouting, as reported previously for epileptic rats (Jiao & Nadler, 2007; but see Jinde et al. 2012). There was no significant correlation between the percent area of black Timm staining and seizure frequency ($R = 0.178$, $p = 0.058$, ANOVA) (Figure 5f).

3.6 No significant correlation between the extent of astrogliosis and seizure frequency

In control mice, GFAP-positive cells were spaced throughout the dentate gyrus (Figure 6a1). The percent area of the dentate gyrus that was GFAP-positive was relatively constant along the septotemporal axis (Figure 6c). In epileptic mice, GFAP-positive cells appeared to be hypertrophied (Figure 6a2). The average percent area of the dentate gyrus that was GFAP-positive in epileptic mice (29.8 ± 0.6%) was 1.5× larger than in control mice (20.1 ± 1.4%, $p < 0.001$, *t* test) (Figure 6b). The average percent area of GFAP-staining was larger in epileptic mice compared to controls at all septotemporal levels (Figure 6c). There was no significant correlation between the percent area that was GFAP-positive and seizure frequency ($R = 0.116$, $p = 0.244$, Spearman rank order correlation) (Figure 6d).

3.7 Significant correlation between the number of GABAergic neurons and seizure frequency

GABAergic interneurons were identified by in situ hybridization for GAD. In control mice, GAD-positive neurons were evident in all layers of the dentate gyrus, especially in the hilus and at the hilar border with the granule cell layer (Figure 7a1). GAD-positive neurons were more abundant in sections from the temporal part of the hippocampus (Figure 7d).

In epileptic mice, the number of GAD-positive neurons appeared to be reduced, especially in the hilus (Figure 7a2), as reported previously for epileptic rats (Obenaus, Esclapez, & Houser, 1993). Surviving GAD-positive neurons in epileptic mice appeared to be stained more intensely than in controls, as described previously for epileptic rats (Feldblum, Ackermann, & Tobin, 1990). The number of GAD-positive neuron profiles was reduced in epileptic mice at all septotemporal levels of the hippocampus, especially in temporal sections (Figure 7d).

There was a high correlation ($R = 0.977$) between the number of GAD-positive profiles counted and the total number of GAD-positive neurons per dentate gyrus estimated by the optical fractionator method in a subset of mice (Figure 7b, Table 1). The slope of the regression line was used to estimate the total number of GAD-positive neurons per dentate gyrus from profile counts for all of the mice. The average number of GAD-positive neurons per hippocampus in control mice was comparable to that estimated in one previous study (Guo, Koshizaki, et al., 2013), but higher than that in another (Wei et al., 2015). The average number of GAD-positive neurons per dentate gyrus in epileptic mice (5660 ± 70) was 72% of that in controls (7860 ± 300, $p < 0.001$, Mann–Whitney rank sum test) (Figure 7c). There was a significant negative correlation between the total number of GAD-positive neurons per dentate gyrus and seizure frequency ($R = 0.199$, $p = 0.029$, ANOVA) (Figure 7e).

To identify the subgroup(s) responsible for the correlation with seizure frequency, GAD-positive neurons were divided based on location, either in the molecular layer, granule cell layer, or hilus. The average number of molecular layer GAD-positive neurons per dentate

gyrus was the same in epileptic mice (1650 ± 30) and controls (1650 ± 60, $p = 0.999$, *t* test) (Figure 7f,g). Similarly, molecular layer GAD-positive neurons are spared in a rat model of temporal lobe epilepsy (Obenaus, Esclapez, & Houser, 1993). There was no significant correlation between the number of molecular layer GAD-positive neurons per dentate gyrus and seizure frequency ($R = 0.129$, $p = 0.160$, ANOVA) (Figure 7h).

The average number of granule cell layer GAD-positive neurons per dentate gyrus in epileptic mice (3050 ± 50) was 77% of that in controls (3960 ± 170, $p < 0.001$, *t* test) (Figure 7i). Loss of granule cell layer GAD neurons was most severe in the temporal part of the hippocampus (Figure 7j). There was a significant negative correlation between the number of granule cell layer GAD-positive neurons per dentate gyrus and seizure frequency ($R = 0.229$, $p = 0.012$, ANOVA) (Figure 7k).

The average number of GAD-positive neurons in the hilus per dentate gyrus of epileptic mice (970 ± 30) was only 43% of that in controls (2250 ± 120, $p \leq 0.001$, Mann–Whitney rank sum test) (Figure 7l). Loss of hilar GAD neurons was most severe in the temporal part of the hippocampus (Figure 7m). There was no significant correlation between the number of hilar GAD-positive neurons per dentate gyrus and seizure frequency ($R = 0.001$, $p = 0.996$, ANOVA) (Figure 7n).

3.8 No significant correlation between the number of parvalbumin-positive interneurons and seizure frequency

Parvalbumin-positive interneurons are one of the subtypes of GABAergic interneurons located in or adjacent to the granule cell layer (Kosaka et al., 1987). There appeared to be fewer parvalbumin-positive neurons in epileptic mice compared to controls (Figure 8a). In control mice, there were more parvalbumin-positive neuron profiles in sections from the temporal part of the hippocampus (Figure 8c). In epileptic mice, most of the loss of parvalbumin-positive neurons was in the middle and temporal parts of the hippocampus.

There was a high correlation ($R = 0.985$) between the number of parvalbumin-positive profiles counted and the number of parvalbumin-positive neurons per dentate gyrus estimated by the optical fractionator method in a subset of mice (Figure 8b, Table 1). The slope of the regression line was used to estimate the total number of parvalbumin-positive neurons per dentate gyrus from the profile counts for all of the mice. The average number of parvalbumin-positive neurons per dentate gyrus in controls was 950 ± 70. That is 12% of the total number of GAD-positive neurons per dentate gyrus. The average number of parvalbumin-positive interneurons per dentate gyrus in epileptic mice (650 ± 10) was 68% of that in controls ($p < 0.001$, *t* test) (Figure 8d). There was no significant correlation between the number of parvalbumin-positive neurons per dentate gyrus and seizure frequency ($R = 0.002$, $p = 0.979$, ANOVA) (Figure 8e).

3.9 Other potential contributors to seizure frequency

Finally, multiple linear regression was performed to test for other potential contributors to seizure frequency, in addition to granule cell layer GAD-positive neuron loss. Multiple linear regression tested whether an association with seizure frequency would be stronger by simultaneously including all of the pathological abnormalities measured in this study. The

correlation coefficient was higher ($R = 0.328$) than that of single regression analyses. However, granule cell layer GAD-positive neuron numbers alone could account for the ability to predict seizure frequency ($p = 0.019$, ANOVA). Percent GFAP ($p = 0.168$), percent Timm staining ($p = 0.478$), number of large GluR2-positive hilar neurons ($p = 0.493$), and number of hilar Prox1-positive neurons ($p = 0.226$) were not necessary to predict seizure frequency with multiple linear regression.

Mice were 28–129 days old (58 ± 2 days) when they were treated with pilocarpine. They were 91–197 days old (129 ± 2 days) when perfused. There was a significant correlation between age and seizure frequency, and it was strongest for age at perfusion ($R = 0.302$, $p < 0.001$, ANOVA) (Figure 9a). Age at perfusion was determined by age at pilocarpine treatment, plus time between pilocarpine treatment and the onset of seizure monitoring, plus duration of seizure monitoring. Duration of seizure monitoring did not vary much (range, 24–36 days, 29 ± 0.2 days), and there was no significant correlation with seizure frequency ($R = -0.169$, $p = 0.061$, Spearman rank order correlation) (Figure 9b). Time between pilocarpine treatment and the onset of seizure monitoring varied more (range, 31–61 days, 42 ± 1 days), and there was a significant correlation with seizure frequency ($R = 0.274$, $p = 0.002$, ANOVA) (Figure 9c). Multiple linear regression was used to test together the correlation of age, time between pilocarpine treatment and seizure monitoring, and number of granule cell layer GAD neurons with seizure frequency. The correlation coefficient ($R = 0.392$) was higher than those with simple regression of the parameters, individually. Seizure frequency could be predicted by a linear combination of perfusion age ($p = 0.014$) and granule cell layer GAD neuron number ($p = 0.013$). Time between pilocarpine treatment and seizure monitoring was not needed to predict seizure frequency ($p = 0.155$).

4 DISCUSSION

The principal finding of this study is that the frequency of spontaneous seizures in epileptic pilocarpine-treated mice correlated with the loss of GABAergic interneurons in or adjacent to the granule cell layer. Seizure frequency did not correlate with the extent of mossy fiber sprouting or astrogliosis, or with the number of hilar ectopic granule cells, mossy cells, parvalbumin interneurons, or GAD neurons in the molecular layer or hilus. These findings prioritize loss of granule cell layer GABAergic interneurons for further testing as a possible cause of temporal lobe epilepsy.

4.1 Correlation between granule cell layer GABAergic neuron loss and seizure frequency

Loss of GABAergic neurons would be expected to reduce inhibition of granule cells. Granule cell inhibition is reduced in patients with temporal lobe epilepsy (Williamson, Patrylo, & Spencer, 1999). Miniature inhibitory postsynaptic currents (mIPSCs) provide a relatively direct measure of inhibition. In several different rodent models of temporal lobe epilepsy, the frequency of mIPSCs recorded in granule cells is substantially reduced compared to controls (Kobayashi & Buckmaster, 2003; Shao & Dudek, 2005; Sun, Mtchedlishvili, Bertram, Erisir, & Kapur, 2007). After transplantation of interneuron precursors into the hippocampus of rodent models of temporal lobe epilepsy, new GABAergic synapses develop with granule cells (Henderson et al., 2014), and seizure

frequency is reduced (Hunt, Girskis, Rubenstein, Alvarez-Buylla, & Baraban, 2013; Waldau, Hattiangady, Kuruba, & Shetty, 2010). These findings are consistent with the hypothesis that loss of granule cell layer GABAergic neurons reduces inhibition of granule cells, which makes seizures more likely to initiate.

The potential epileptogenic role of granule cell layer GABAergic neuron loss in temporal lobe epilepsy remains uncertain, however. This study tested for correlation, but did not establish causality. Some investigators might question the assumption that if a pathological abnormality were epileptogenic, then its severity should correlate with seizure frequency. We believe the assumption is reasonable and could not identify a more reliable metric of epileptogenicity.

The extent to which granule cell layer GABAergic neuron loss occurs in patients is unclear. Previous human studies that used GAD-immunocytochemistry as a general marker of interneurons reported values in epileptic patients not significantly lower than in controls (Babb et al., 1989; Mathern et al., 1995). However, those studies had limitations. Interneurons were measured as a function of tissue volume or as a percentage of Nissl stained neurons. Therefore, interneuron loss could occur without detection, because of corresponding reductions in volume or total number of neurons. Furthermore, tissue preservation and control groups were not ideal. In addition, GAD-immunocytochemistry fails to label all GABAergic neurons in the dentate gyrus (Houser, 2007). Studies that used markers of specific inter-neuron subtypes that tend to be positioned in or adjacent to the granule cell layer reported fewer interneurons in tissue from patients (Maglóczky et al., 2000; Tóth et al., 2010). Therefore, it is possible that in patients with temporal lobe epilepsy, the total number of GABAergic interneurons in the granule cell layer is reduced.

The correlation between granule cell layer GABAergic neuron loss and seizure frequency was significant, but weak ($R = 0.229$). Huusko, Römer, Ndode-Ekane, Lukasiuk, and Pitkänen (2015) reported more severe loss of dentate gyrus interneurons, but fewer seizures after traumatic brain injury versus electrical stimulation of the amygdala. However, there could be other differences after traumatic brain injury versus amygdalar stimulation that confound the comparison of the effects of interneuron loss.

In this study, time-saving methods were used, because of the large sample size and laborious nature of the analyses. Some elements of the experimental design may have reduced the correlation between seizure frequency and interneuron loss. For example, our study did not count all of the seizures that occurred during the monitoring period, and seizure frequency was based only on behavioral monitoring. Previous studies indicate that >90% of electrographic seizures are accompanied by behavioral convulsions in this model (Buckmaster & Lew, 2011; Hester & Danzer, 2013; Mazzuferi et al., 2012). Seizure monitoring was only 9 hr/day, not 24 hr/day. Continuous monitoring with video and electroencephalography would have generated more accurate results. In addition, only one hippocampus was examined per mouse. Specific, focal sites of seizure initiation were not identified and analyzed selectively for pathological abnormalities in individual subjects.

Furthermore, we examined only a subset of the pathological abnormalities that occur in patients with temporal lobe epilepsy. It is possible that other abnormalities correlate more strongly with seizure frequency. The dentate gyrus has been proposed to function like a gate that normally prevents excessive synaptic input from propagating into downstream hippocampal areas (Heinemann et al., 1992). Therefore, pathological abnormalities in upstream brain regions—including the amygdala, olfactory cortex, and entorhinal cortex—might contribute to seizure frequency. However, in epileptic pilocarpine-treated rats, most seizures appear to initiate in the hippocampal formation (Toyoda, Bower, Leyva, & Buckmaster, 2013).

In this study, mice were treated with pilocarpine when they were at a range of ages. Older mice tended to have higher seizure frequencies. Similarly, rats are more likely to develop epilepsy when they experience pilocarpine-induced status epilepticus as adults versus juveniles (Priel, Ferreira dos Santos, & Cavalheiro, 1996). Spontaneous motor seizures eventually developed in all rats treated with pilocarpine at 50 days of age or older, but in none treated at 17 days old or younger. Our mice were treated with pilocarpine when they were 28–192 days old. Future studies might reduce variability in seizure frequency by standardizing subject age and time between pilocarpine treatment and seizure monitoring.

Despite the limitations and caveats discussed above, seizure frequency correlated with loss of GAD neurons in the granule cell layer. Parvalbumin-positive basket cells are the best characterized interneurons associated with the granule cell layer (Hu, Gan, & Jonas, 2014). In patients with temporal lobe epilepsy, fewer parvalbumin-positive basket cells are found in the dentate gyrus (Andrioli, Alonso-Nanclares, Arellano, & DeFilipe, 2007). However, the loss might be attributable to reduced immunoreactivity, instead of cell death (Sloviter, Sollas, Barbaro, & Laxer, 1991; Wittner et al., 2001). In this study, no significant correlation was found between the loss of parvalbumin-positive inter-neurons and seizure frequency. Other interneuron subtypes, besides parvalbumin neurons, are located in or adjacent to the granule cell layer. Some do not appear to be reduced in models of temporal lobe epilepsy, including cholecystokinin- (Sun et al., 2007) and NADPH-diaphorase-positive interneurons (Hamani, Tenório, Mendez-Otero, & Mello, 1999; Kotti, Halonen, Sirviö, Riekkinen, & Miettinen, 1997). However, the loss of other subtypes of interneurons might correlate with seizure frequency. They include calretinin-positive interneurons (Megías, Verduga, Fernández-Viadero, & Crespo, 1997), COUP-TFII-positive interneurons (Fuentealba et al., 2010), and molecular layer-projecting interneurons (Soriano & Frotscher, 1993; Yu, Swietek, Proddutur, & Santhakumar, 2015). To further test the hypothesis, it would be useful to identify the vulnerable interneurons and determine whether their selective loss is epileptogenic.

4.2 No significant correlation between other pathological abnormalities and seizure frequency

No significant correlation was found between the number of hilar ectopic granule cells and seizure frequency. Mice with deletion of Bcl-2-associated X protein (BAX) (Myers, Bermudez-Hernandez, & Scharfman, 2013) or disabled-1 genes (Korn, Mandle, & Parent, 2016) develop hilar ectopic granule cells, but not epilepsy. Similarly, mice treated with

phenobarbital at a young age develop hilar ectopic granule cells, but not epilepsy (Koyama et al., 2012). Together, these findings suggest hilar ectopic granule cells are not epileptogenic.

Several studies reported a significant correlation between the number of hilar ectopic granule cells and seizure frequency. In those studies, however, seizure monitoring methods were limited (McCloskey et al., 2006), sample size was small (Hester & Danzer, 2013), or correlations were inconsistent depending on experimental conditions (Koyama et al., 2012). Our data came from a large sample using optical fractionator cell counting methods. Our findings suggest that associations between seizure frequency and neurogenesis (Cho et al., 2015; Hosford, Liska, & Danzer, 2016; Jung et al., 2004) are attributable to factors other than hilar ectopic granule cells.

No significant correlation was found between mossy cell loss and seizure frequency. Ratzliff, Howard, Santhakumar, Osapay, & Soltesz (2004) reported that deletion of mossy cells reduces excitability of granule cells. Jinde et al. (2012) reported no seizures after deletion of mossy cells. Together, these findings suggest mossy cell loss is not epileptogenic. Furthermore, the lack of correlation between the number of surviving mossy cells and seizure frequency suggests they do not become super-connected ictogenic hub cells.

Most previous studies found no significant correlation between the extent of mossy fiber sprouting and seizure frequency (reviewed in Buckmaster, 2012). Results of this study are consistent. A variety of experimental manipulations also reveal disassociation between mossy fiber sprouting and epileptogenesis (Buckmaster & Lew, 2011; Cho et al., 2015; Guo, Zeng, Brody, & Wong, 2013; Heng et al., 2013; Hosford et al., 2016; Pun et al., 2012). Consequently, mossy fiber sprouting does not appear to be epileptogenic.

Seizure activity causes astrogliosis in the dentate gyrus (Bonthius, Stringer, Lothman, & Steward, 1994). Astrogliosis found in patients with temporal lobe epilepsy is replicated in animal models (Bendotti, Guglielmetti, Tortarolo, Samanin, & Hirst, 2000; Garzillo & Mello, 2002), including pilocarpine-treated mice (Borges, McDermott, Irier, Smith, & Dingledine, 2006). Robel et al. (2015) conditionally deleted β1-integrin in mice, which caused astrogliosis throughout the brain, without other pathologies. Those mice displayed spontaneous seizures, suggesting astrogliosis alone can be epileptogenic. In this study, the average GFAP-positive area in the dentate gyrus of epileptic mice was 1.5× larger than in control mice, but there was no significant correlation with seizure frequency. In β1-integrin deficient mice, GFAP-positive area was >5× larger than in controls. These findings suggest that the extent of astrogliosis in epileptic pilocarpine-treated mice is not sufficient to cause seizures.

The loss of hilar GABAergic neurons was extensive in epileptic mice. Somatostatin-positive hilar interneurons inhibit granule cells at the dendritic level (Buckmaster, Yamawaki, & Zhang, 2002; Leranth, Malcolm, & Frotscher, 1990) and account for more than half of hilar GABAergic neurons (Austin & Buckmaster, 2004). Their loss in patients with temporal lobe epilepsy (de Lanerolle et al., 1989; Mathern et al., 1995) is replicated in animal models (Buckmaster & Dudek, 1997; Gorter, van Vliet, Aronica, & Lopes da Silva, 2001;

Schwarzer, Williamson, Lothman, Vezzani, & Sperk, 1995; Sperk et al., 1992; Sun et al., 2007). Hilar somatostatin interneuron loss can reduce inhibitory control of granule cells (Hofmann, Balgooyen, Mattis, Deisseroth, & Buckmaster, 2016). The surprising lack of correlation between the number of hilar GAD-positive neurons per dentate gyrus and seizure frequency was definitive ($R = 0.001$, $p = 0.996$, ANOVA). Therefore, there was little rationale for counting somatostatin interneurons, which would have been laborious and probably futile. Compensatory axon sprouting by surviving somatostatin interneurons (Peng et al., 2013; Thind et al., 2010; Zhang et al., 2009) could explain the lack of correlation between seizure frequency and the loss of hilar GABAergic neurons.

The mechanisms of temporal lobe epilepsy remain unclear. Many possibilities have been proposed. It is challenging for investigators to decide how to invest their efforts and resources in search of underlying causes of temporal lobe epilepsy. Results of this study suggest hilar ectopic granule cells, mossy cells, mossy fiber sprouting, astrogliosis, and the loss of parvalbumin-positive interneurons and GABAergic interneurons in the molecular layer and hilus have lower priority for further evaluation. Instead, loss of granule cell layer GABAergic inter-neurons appears to be worthy of further testing as a potential epileptogenic mechanism.

Acknowledgments

Funding information

NINDS/NIH, Grant/Award Number: NS039110 and NS040276

The authors are grateful to Yui Yin Chu for technical assistance.

References

Andrioli A, Alonso-Nanclares L, Arellano JI, DeFilipe J. Quantitative analysis of parvalbumin-immunoreactive cells in the human epileptic hippocampus. Neuroscience. 2007; 149:131–143. [PubMed: 17850980]

Austin JE, Buckmaster PS. Recurrent excitation of granule cells with basal dendrites and low interneuron density and inhibitory postsynaptic current frequency in the dentate gyrus of macaque monkeys. The Journal of Comparative Neurology. 2004; 476:205–218. [PubMed: 15269966]

Babb TL, Brown WJ, Pretorius J, Davenport C, Lieb JP, Crandall PH. Temporal lobe volumetric cell densities in temporal lobe epilepsy. Epilepsia. 1984; 25:729–740. [PubMed: 6510381]

Babb TL, Kupfer WR, Pretorius JK, Crandall PH, Levesque MF. Synaptic reorganization by mossy fibers in human epileptic fascia dentata. Neuroscience. 1991; 42:351–363. [PubMed: 1716744]

Babb TL, Pretorius JK, Kupfer WR, Crandall PH. Glutamate decarboxylase-immunoreactive neurons are preserved in human epileptic hippocampus. The Journal of Neuroscience. 1989; 9:2562–2574. [PubMed: 2501460]

Bendotti C, Guglielmetti F, Tortarolo M, Samanin R, Hirst WD. Differential expression of S100β and glial fibrillary acidic protein in the hippocampus after kainic acid-induced lesions and mossy fiber sprouting in adult rat. Experimental Neurology. 2000; 161:317–329. [PubMed: 10683297]

Binder DK, Steinhäuser C. Functional changes in astroglial cells in epilepsy. Glia. 2006; 54:358–368. [PubMed: 16886201]

Blümcke I, Zuschratter W, Schewe JC, Suter B, Lie AA, Riederer BM, … Wiestler OD. Cellular pathology of hilar neurons in Ammon's horn sclerosis. The Journal of Comparative Neurology. 1999; 414:437–453. [PubMed: 10531538]

Boison D. Adenosinergic signaling in epilepsy. Neuropharmacology. 2016; 104:131–139. [PubMed: 26341819]

Bonthius DJ, Stringer JL, Lothman EW, Steward O. Spreading depression and reverberatory seizures induce the upregulation of mRNA for glial fibrillary acidic protein. Brain Research. 1994; 645:215–224. [PubMed: 8062084]

Borges K, McDermott D, Irier H, Smith Y, Dingledine R. Degeneration and proliferation of astrocytes in the mouse dentate gyrus after pilocarpine-induced status epilepticus. Experimental Neurology. 2006; 201:416–427. [PubMed: 16793040]

Bouilleret V, Ridoux V, Depaulis A, Marescaux C, Nehlig A, Le Gal La Salle G. Recurrent seizures and hippocampal sclerosis following intrahippocampal kainate injection in adult mice: Electroencephalography, histopathology and synaptic reorganization similar to mesial temporal lobe epilepsy. Neuroscience. 1999; 89:717–729. [PubMed: 10199607]

Buckmaster, PS. Mossy fiber sprouting in the dentate gyrus. Jasper's basic mechanisms of the epilepsies. 4. New York, NY: Oxford University Press; 2012.

Buckmaster PS, Dudek FE. Neuron loss, granule cell axon reorganization, and functional changes in the dentate gyrus of epileptic kainate-treated rats. The Journal of Comparative Neurology. 1997; 385:385–404. [PubMed: 9300766]

Buckmaster PS, Lew FH. Rapamycin suppresses mossy fiber sprouting but not seizure frequency in a mouse model of temporal lobe epilepsy. The Journal of Neuroscience. 2011; 31:2337–2347. [PubMed: 21307269]

Buckmaster PS, Yamawaki R, Zhang GF. Axon arbors and synaptic connections of a vulnerable population of interneurons in the dentate gyrus in vivo. The Journal of Comparative Neurology. 2002; 445:360–373. [PubMed: 11920713]

Buhl EH, Otis TS, Mody I. Zinc-induced collapse of augmented inhibition by GABA in a temporal lobe epilepsy model. Science. 1996; 271:369–373. [PubMed: 8553076]

Cameron MC, Zhan R, Nadler JV. Morphologic integration of hilar ectopic granule cells into dentate gyrus circuitry in the pilocarpine model of temporal lobe epilepsy. The Journal of Comparative Neurology. 2011; 519:2175–2192. [PubMed: 21455997]

Cho K, Lybrand ZR, Ito N, Brulet R, Tafacory F, Zhang L, … Hsieh J. Aberrant hippocampal neurogenesis contributes to epilepsy and associated cognitive decline. Nature Communications. 2015; 6:6606.

Clasadonte J, Dong J, Hines DJ, Haydon PG. Astrocyte control of synaptic NMDA receptors contributes to the progressive development of temporal lobe epilepsy. Proceedings of the National Academy of Sciences of the United States of America. 2013; 110:17540–17545. [PubMed: 24101472]

Dam AM. Epilepsy and neuron loss in the hippocampus. Epilepsia. 1980; 21:617–629. [PubMed: 6777154]

Das A, Wallace GC, Holmes C, McDowell ML, Smith JA, Marshall JD, … Banik NL. Hippocampal tissue of patients with refractory temporal lobe epilepsy is associated with astrocyte activation, inflammation, and altered expression of channels and receptors. Neuroscience. 2012; 220:237–246. [PubMed: 22698689]

de Lanerolle NC, Kim JH, Robbins RJ, Spencer DD. Hippocampal interneuron loss and plasticity in human temporal lobe epilepsy. Brain Research. 1989; 495:387–395. [PubMed: 2569920]

Erlander MG, Tillakaratne NJK, Feldblum S, Patel N, Tobin AJ. Two genes encode distinct glutamate decarboxylases. Neuron. 1991; 7:91–100. [PubMed: 2069816]

Feldblum S, Ackermann RF, Tobin AJ. Long-term increase of glutamate decarboxylase mRNA in a rat model of temporal lobe epilepsy. Neuron. 1990; 5:361–371. [PubMed: 1976015]

Franck JE, Pokorny J, Kunkel DD, Schwartzkroin PA. Physiologic and morphologic characteristics of granule cell circuitry in human epileptic hippocampus. Epilepsia. 1995; 36:543–558. [PubMed: 7555966]

Fuentealba P, Klausberger T, Karayannis T, Suen WY, Huck J, Tomioka R, … Somogyi P. Expression of COUP-TFII nuclear receptor in restricted GABAergic neuronal populations in the adult rat hippocampus. The Journal of Neuroscience. 2010; 30:1595–1609. [PubMed: 20130170]

Fujise N, Kosaka T. Mossy cells in the mouse dentate gyrus: Identification in the dorsal hilus and their distribution along the dorsoventral axis. Brain Research. 1999; 816:500–511. [PubMed: 9878875]

Fujise N, Liu Y, Hori N, Kosaka T. Distribution of calretinin immunoreactivity in the mouse dentate gyrus: II. Mossy cells, with special reference to their dorsoventral difference in calretinin immunoreactivity. Neuroscience. 1998; 82:181–200. [PubMed: 9483514]

Gabriel S, Njunting M, Pomper JK, Merschhemke M, Sanabria ER, Eilers A, … Lehmann TN. Stimulus and potassium-induced epileptiform activity in the human dentate gyrus from patients with and without hippocampal sclerosis. The Journal of Neuroscience. 2004; 24:10416–10430. [PubMed: 15548657]

Garzillo CL, Mello LEAM. Characterization of reactive astrocytes in the chronic phase of the pilocarpine model of epilepsy. Epilepsia. 2002; 43(Suppl 5):107–109.

Gibbons MB, Smeal RM, Takahashi DK, Vargas JR, Wilcox KS. Contributions of astrocytes to epileptogenesis following status epilepticus: Opportunities for preventive therapy? Neurochemistry International. 2013; 63:660–669. [PubMed: 23266599]

Goelz MF, Mahler J, Harry J, Myers P, Clark J, Thigpen JE, Forsyth DB. Neuropathologic findings associated with seizures in FVB mice. Laboratory Animal Science. 1998; 48:34–37. [PubMed: 9517887]

Gorter JA, van Vliet EA, Aronica E, Lopes da Silva FH. Progression of spontaneous seizures after status epilepticus is associated with mossy fibre sprouting and extensive bilateral loss of hilar parvalbumin and somatostatin-immunoreactive neurons. The European Journal of Neuroscience. 2001; 13:657–669. [PubMed: 11207801]

Guo D, Zeng L, Brody DL, Wong M. Rapamycin attenuates the development of posttraumatic epilepsy in a mouse model of traumatic brain injury. PLoS One. 2013; 8:e64078. [PubMed: 23691153]

Guo N, Koshizaki K, Kimura R, Suto F, Yanagawa Y, Osumi N. A sensitive period for GABAergic interneurons in the dentate gyrus in modulating sensorimotor gating. The Journal of Neuroscience. 2013; 33:6691–6704. [PubMed: 23575865]

Hamani C, Tenório F, Mendez-Otero R, Mello LEAM. Loss of NADPH diaphorase-positive neurons in the hippocampal formation of chronic pilocarpine-epileptic rats. Hippocampus. 1999; 9:303–313. [PubMed: 10401644]

Hanbury R, Ling ZD, Wuu J, Kordower JH. GFAP knockout mice have increased levels of GDNF that protect striatal neurons from metabolic and excitotoxic insults. The Journal of Comparative Neurology. 2003; 461:307–316. [PubMed: 12746870]

Heinemann U, Beck H, Dreier JP, Ficker E, Stabel J, Zhang CL. The dentate gyrus as a regulated gate for the propagation of epileptiform activity. Epilepsy Research Supplement. 1992; 7:273–280. [PubMed: 1334666]

Henderson KW, Gupta J, Tagliatela S, Litvina E, Zheng XT, Van Zandt MAV, … Naegele JR. Long-term seizure suppression and optogenetic analyses of synaptic connectivity in epileptic mice with hippocampal grafts of GABAergic interneurons. The Journal of Neuroscience. 2014; 34:13492–13504. [PubMed: 25274826]

Heng K, Haney MM, Buckmaster PS. High-dose rapamycin blocks mossy fiber sprouting but not seizures in a mouse model of temporal lobe epilepsy. Epilepsia. 2013; 54:1535–1541. [PubMed: 23848506]

Hester MS, Danzer SC. Accumulation of abnormal adult-generated hippocampal granule cells predicts seizure frequency and severity. The Journal of Neuroscience. 2013; 33:8926–8936. [PubMed: 23699504]

Hofmann G, Balgooyen L, Mattis J, Deisseroth K, Buckmaster PS. Hilar somatostatin interneuron loss reduces dentate gyrus inhibition in a mouse model of temporal lobe epilepsy. Epilepsia. 2016; 57:977–983. [PubMed: 27030321]

Hosford BE, Liska JP, Danzer SC. Ablation of newly generated hippocampal granule cells has disease-modifying effects in epilepsy. The Journal of Neuroscience. 2016; 36:11013–11023. [PubMed: 27798182]

Houser CR. Granule cell dispersion in the dentate gyrus of humans with temporal lobe epilepsy. Brain Research. 1990; 535:195–204. [PubMed: 1705855]

Houser CR. Interneurons of the dentate gyrus: An overview of cell types, terminal fields and neurochemical identity. Progress in Brain Research. 2007; 163:217–232. [PubMed: 17765721]

Houser CR, Miyashiro JE, Swartz BE, Walsh GO, Rich JR, Delgado-Escueta AV. Altered patterns of dynorphin immunoreactivity suggest mossy fiber reorganization in human hippocampal epilepsy. The Journal of Neuroscience. 1990; 10:267–282. [PubMed: 1688934]

Hu H, Gan J, Jonas P. Fast-spiking, parvalbumin + GABAergic interneurons: From cellular design to microcircuit function. Science. 2014; 345:1255263. [PubMed: 25082707]

Hubbard JA, Szu JI, Yonan JM, Binder DK. Regulation of astrocyte glutamate transporter-1 (GLT1) and aquaporin-4 (AQP4) expression in a model of epilepsy. Experimental Neurology. 2016; 283:85–96. [PubMed: 27155358]

Hunt RF, Girskis KM, Rubenstein JL, Alvarez-Buylla A, Baraban SC. GABA progenitors grafted into the adult epileptic brain control seizures and abnormal behaviors. Nature Neuroscience. 2013; 16:692–697. [PubMed: 23644485]

Huusko N, Römer C, Ndode-Ekane XE, Lukasiuk K, Pitkänen A. Loss of hippocampal interneurons and epileptogenesis: A comparison of two animal models of acquired epilepsy. Brain Structure & Function. 2015; 220:153–191. [PubMed: 24096381]

Jiao Y, Nadler JV. Stereological analysis of GluR2-immunoreactive hilar neurons in the pilocarpine model of temporal lobe epilepsy: Correlation of cell loss with mossy fiber sprouting. Experimental Neurology. 2007; 205:569–582. [PubMed: 17475251]

Jinde S, Zsiros V, Jiang Z, Nakao K, Pickel J, Kohno K, … Nakazawa K. Hilar mossy cell degeneration causes transient dentate granule cell hyperexcitability and impaired pattern separation. Neuron. 2012; 76:1189–1200. [PubMed: 23259953]

Johnson AM, Sugo E, Barreto D, Hiew C, Lawson JA, Connolly AM, … Cunningham AM. The severity of gliosis in hippocampal sclerosis correlates with pre-operative seizure burden and outcome after temporal lobectomy. Molecular Neurobiology. 2016; 53:5446–5456. [PubMed: 26452360]

Jung K, Chu K, Kim M, Jeong S, Song Y, Lee S, … Roh J. Continuous cytosine-b-D-arabinofuranoside infusion reduces ectopic granule cells in adult rat hippocampus with attenuation of spontaneous recurrent seizures following pilocarpine-induced status epilepticus. The European Journal of Neuroscience. 2004; 19:3219–3226. [PubMed: 15217378]

Kobayashi M, Buckmaster PS. Reduced inhibition of dentate granule cells in a model of temporal lobe epilepsy. The Journal of Neuroscience. 2003; 23:2440–2452. [PubMed: 12657704]

Korn MJ, Mandle QJ, Parent JM. Conditional disabled-1 deletion in mice alters hippocampal neurogenesis and reduces seizure threshold. Frontiers in Neuroscience. 2016; 10:63. [PubMed: 26941603]

Kosaka T, Katsumaru H, Hama K, Wu JY, Heizmann CW. GABAergic neurons containing the Ca2+-binding protein parvalbumin in the rat hippocampus and dentate gyrus. Brain Research. 1987; 419:119–130. [PubMed: 3315112]

Kotti T, Halonen T, Sirviö J, Riekkinen P, Miettinen R. Comparison of NADPH diaphorase histochemistry, somatostatin immunohistochemistry, and silver impregnation in detecting structural and functional impairment in experimental status epilepticus. Neuroscience. 1997; 80:105–117. [PubMed: 9252225]

Koyama R, Tao K, Sasaki T, Ichikawa J, Miyamoto D, Muramatsu R, … Ikegaya Y. GABAergic excitation after febrile seizures induces ectopic granule cells and adult epilepsy. Nature Medicine. 2012; 18:1271–1278.

Lavado A, Lagutin OV, Chow LM, Baker SJ, Oliver G. Prox1 is required for granule cell maturation and intermediate progenitor maintenance during brain neurogenesis. PLoS Biology. 2010; 8:e1000460. [PubMed: 20808958]

Leranth C, Malcolm AJ, Frotscher M. Afferent and efferent synaptic connections of somatostatin-immunoreactive neurons in the rat fascia dentata. The Journal of Comparative Neurology. 1990; 295:111–122. [PubMed: 1971287]

Leranth C, Szeidemann Z, Hsu M, Buzsáki G. AMPA receptors in the rat and primate hippocampus: A possible absence of GluR2/3 subunits in most interneurons. Neuroscience. 1996; 70:631–52. [PubMed: 9045077]

Lew FH, Buckmaster PS. Is there a critical period for mossy fiber sprouting in a mouse model of temporal lobe epilepsy? Epilepsia. 2011; 52:2326–2332. [PubMed: 22092282]

Liu M, Pleasure SJ, Collins AE, Noebels JL, Naya FJ, Tsai MJ, Lowenstein DH. Loss of BETA2/NeuroD leads to malformation of the dentate gyrus and epilepsy. Proceedings of the National Academy of Sciences of the United States of America. 2000; 97:865–870. [PubMed: 10639171]

Magloczky Z, Wittner L, Borhegyi Z, Halász P, Vajda J, Czirják S, Freund TF. Changes in the distribution and connectivity of inter-neurons in the epileptic human dentate gyrus. Neuroscience. 2000; 96:7–25. [PubMed: 10683405]

Mahler JF, Stokes W, Mann PC, Takaoka M, Maronpot RR. Spontaneous lesions in aging FVB/N mice. Toxicologic Pathology. 1996; 24:710–716. [PubMed: 8994298]

Margerison JH, Corsellis JAN. Epilepsy and the temporal lobes. Brain. 1966; 89:499–530. [PubMed: 5922048]

Maroso M, Balosso S, Ravizza T, Liu J, Aronica E, Iyer AM, … Vezzani A. Toll-like receptor 4 and high-mobility group box-1 are involved in ictogenesis and can be targeted to reduce seizures. Nature Medicine. 2010; 16:413–419.

Masukawa LM, O'Connor WM, Lynott J, Burdette LJ, Uruno K, McGonigle P, O'Connor MJ. Longitudinal variation in cell density and mossy fiber reorganization in the dentate gyrus from temporal lobe epileptic patients. Brain Research. 1995; 678:65–75. [PubMed: 7620900]

Masukawa LM, Wang H, O'Connor MJ, Uruno K. Prolonged field potentials evoked by 1 Hz stimulation in the dentate gyrus of temporal lobe epileptic human brain slices. Brain Research. 1996; 721:132–139. [PubMed: 8793093]

Mathern GW, Babb TL, Pretorius JK, Leite JP. Reactive synaptogenesis and neuron densities for neuropeptide Y, somatostatin, and glutamate decarboxylase immunoreactivity in the epileptogenic human fascia dentata. The Journal of Neuroscience. 1995; 15:3990–4004. [PubMed: 7751960]

Mazzuferi M, Kumar G, Rospo C, Kaminski RM. Rapid epileptogenesis in the mouse pilocarpine model: Video-EEG, pharmacokinetic and histopathological characterization. Experimental Neurology. 2012; 238:156–167. [PubMed: 22960187]

McCloskey DP, Hintz TM, Pierce JP, Scharfman HE. Stereological methods reveal the robust size and stability of ectopic hilar granule cells after pilocarpine-induced status epilepticus in the adult rat. The European Journal of Neuroscience. 2006; 24:2203–2210. [PubMed: 17042797]

Megías M, Verduga R, Fernández-Viadero C, Crespo D. Neurons co-localizing calretinin immunoreactivity and reduced nicotinamide adenine dinucleotide phosphate diaphorase (NADPH-d) activity in the hippocampus and dentate gyrus of the rat. Brain Research. 1997; 744:112–120. [PubMed: 9030419]

Myers CE, Bermudez-Hernandez K, Scharfman HE. The influence of ectopic migration of granule cells into the hilus on dentate gyrus-CA3 function. PLoS One. 2013; 8:e68208. [PubMed: 23840835]

Nadler JV, Perry BW, Cotman CW. Selective reinnervation of hippocampal area CA1 and the fascia dentata after destruction of CA3-CA4 afferents with kainic acid. Brain Research. 1980; 182:1–9. [PubMed: 7350980]

Obenaus A, Esclapez M, Houser CR. Loss of glutamate decarboxylase mRNA-containing neurons in the rat dentate gyrus following pilocarpine-induced seizures. The Journal of Neuroscience. 1993; 13:4470–4485. [PubMed: 8410199]

Oberheim NA, Tian G, Han X, Peng W, Takano T, Ransom B, Nedergaard M. Loss of astrocytic domain organization in the epileptic brain. The Journal of Neuroscience. 2008; 28:3264–3276. [PubMed: 18367594]

Ortinski PI, Dong J, Mungenast A, Yue C, Takano J, Watson DJ, … Coulter DA. Selective induction of astrocytic gliosis generates deficits in neuronal inhibition. Nature Neuroscience. 2010; 13:584–591. [PubMed: 20418874]

Parent JM, Elliott RC, Pleasure SJ, Barbaro NM, Lowenstein DH. Aberrant seizure-induced neurogenesis in experimental temporal lobe epilepsy. Annals of Neurology. 2006; 59:81–91. [PubMed: 16261566]

Peng Z, Zhang N, Wei W, Huang CS, Cetina Y, Otis TS, Houser CR. A reorganized GABAergic circuit in a model of epilepsy: Evidence from optogenetic labeling and stimulation of somatostatin interneurons. The Journal of Neuroscience. 2013; 33:14392–14405. [PubMed: 24005292]

Priel MR, Ferreira dos Santos N, Cavalheiro EA. Developmental aspects of the pilocarpine model of epilepsy. Epilepsy Research. 1996; 28:115–121.

Pun RYK, Rolle IJ, LaSarge CL, Hosford BE, Rosen JM, Uhl JD, … Danzer SC. Excessive activation of mTOR in post-natally generated granule cells is sufficient to cause epilepsy. Neuron. 2012; 75:1022–1034. [PubMed: 22998871]

Quesney LF. Clinical and EEG features of complex partial seizures of temporal lobe origin. Epilepsia. 1986; 27(Suppl 2):S27–S45.

Racine RJ. Modification of seizure activity by electrical stimulation: II. Motor seizure. Electroencephalography and Clinical Neurophysiology. 1972; 32:281–294. [PubMed: 4110397]

Ratzliff AH, Howard AL, Santhakumar V, Osapay I, Soltesz I. Rapid deletion of mossy cells does not result in a hyperexcitable dentate gyrus: Implications for epileptogenesis. The Journal of Neuroscience. 2004; 24:2259–2369. [PubMed: 14999076]

Ratzliff AH, Santhakumar V, Howard A, Soltesz I. Mossy cells in epilepsy: Rigor mortis or vigor mortis? Trends in Neuroscience. 2002; 25:140–144.

Robel S, Buckingham SC, Boni JL, Campbell SL, Danbolt NC, Riedemann T, … Sontheimer H. Reactive astrogliosis causes the development of spontaneous seizures. The Journal of Neuroscience. 2015; 35:3330–3345. [PubMed: 25716834]

Robel S, Sontheimer H. Glia as drivers of abnormal neuronal activity. Nature Neuroscience. 2016; 19:28–33. [PubMed: 26713746]

Rosenbaum MD, VandeWoude S, Bielefeldt-Ohmann H. Sudden onset of mortality within a colony of FVB/n mice. Lab Animal. 2007; 36:15–16.

Santhakumar V, Bender R, Frotscher M, Ross ST, Hollrigel GS, Toth Z, Soltesz I. Granule cell hyperexcitability in the early post-traumatic rat dentate gyrus: The 'irritable mossy cell' hypothesis. The Journal of Physiology. 2000; 524:117–134. [PubMed: 10747187]

Scharfman HE, Pierce JP. New insights into the role of hilar ectopic granule cells in the dentate gyrus based on quantitative anatomic analysis and three-dimensional reconstruction. Epilepsia. 2012; 53(Suppl 1):98–108.

Scharfman HE, Smith KL, Goodman JH, Sollas AL. Survival of dentate hilar mossy cells after pilocarpine-induced seizures and their synchronized burst discharges with area CA3 pyramidal cells. Neuroscience. 2001; 104:741–759. [PubMed: 11440806]

Schwarzer C, Williamson JM, Lothman EW, Vezzani A, Sperk G. Somatostatin, neuropeptide Y, neurokinin B, and cholecystokinin immunoreactivity in two chronic models of temporal lobe epilepsy. Neuroscience. 1995; 69:831–845. [PubMed: 8596652]

Seress L, Ábrahám H, Horváth Z, Dóczi T, Janszky J, Klemm J, … Bakay RAE. Survival of mossy cells of the hippocampal dentate gyrus in humans with mesial temporal lobe epilepsy. The Journal of Neurosurgery. 2009; 111:1237–1247. [PubMed: 19392605]

Shao LR, Dudek FE. Changes in mIPSCs and sIPSCs after kainate treatment: Evidence for loss of inhibitory input to dentate granule cells and possible compensatory responses. The Journal of Neurophysiology. 2005; 94:952–960. [PubMed: 15772233]

Sloviter RS. Decreased hippocampal inhibition and a selective loss of interneurons in experimental epilepsy. Science. 1987; 235:73–76. [PubMed: 2879352]

Sloviter RS. The functional organization of the hippocampal dentate gyrus and its relevance to the pathogenesis of temporal lobe epilepsy. Annals of Neurology. 1994; 35:640–654. [PubMed: 8210220]

Sloviter RS, Sollas AL, Barbaro NM, Laxer KD. Calcium-binding protein (calbindin-D28K) and parvalbumin immunocytochemistry in the normal and epileptic human hippocampus. The Journal of Comparative Neurology. 1991; 308:381–396. [PubMed: 1865007]

Sloviter RS, Zappone CA, Harvey BD, Bumanglag AV, Bender RA, Frotscher M. "Dormant basket cell" hypothesis revisited: Relative vulnerabilities of dentate gyrus mossy cells and inhibitory interneurons after hippocampal status epilepticus in the rat. The Journal of Comparative Neurology. 2003; 459:44–76. [PubMed: 12629666]

Soriano E, Frotscher M. GABAergic innervation of the rat fascia dentata: A novel type of interneuron in the granule cell layer with extensive axonal arborization in the molecular layer. The Journal of Comparative Neurology. 1993; 334:385–396. [PubMed: 8376624]

Spanedda F, Cendes F, Gotman J. Relations between EEG seizure morphology, interhemispheric spread, and mesial temporal atrophy in bitemporal epilepsy. Epilepsia. 1997; 38:1300–1314. [PubMed: 9578526]

Spencer SS, Williamson PD, Spencer DD, Mattson RH. Human hippocampal seizure spread studied by depth and subdural recording: The hippocampal commissure. Epilepsia. 1987; 28:479–489. [PubMed: 3653050]

Sperk G, Marksteiner J, Gruber B, Bellmann R, Mahata M, Ortler M. Functional changes in neuropeptide Y- and somatostatin-containing neurons induced by limbic seizures in the rat. Neuroscience. 1992; 50:831–846. [PubMed: 1360155]

Sperling MR, O'Connor MJ. Comparison of depth and sub-dural electrodes in recording temporal lobe seizures. Neurology. 1989; 39:1497–1504. [PubMed: 2812330]

Sun C, Mtchedlishvili Z, Bertram EH, Erisir A, Kapur J. Selective loss of dentate hilar interneurons contributes to reduced synaptic inhibition of granule cells in an electrical stimulation-based animal model of temporal lobe epilepsy. The Journal of Comparative Neurology. 2007; 500:876–893. [PubMed: 17177260]

Sutula T, Cascino G, Cavazos J, Parada I, Ramirez L. Mossy fiber synaptic reorganization in the epileptic human temporal lobe. Annals of Neurology. 1989; 26:321–330. [PubMed: 2508534]

Tang FR, Chia SC, Zhang S, Chen PM, Gao H, Liu CP, … Lee WL. Glutamate receptor 1-immunopositive neurons in the gliotic CA1 area of the mouse hippocampus after pilocarpine-induced status epilepticus. The European Journal of Neuroscience. 2005; 21:2361–2374. [PubMed: 15932595]

Tauck DL, Nadler JV. Evidence of functional mossy fiber sprouting in hippocampal formation of kainic acid-treated rats. The Journal of Neuroscience. 1985; 5:1016–1022. [PubMed: 3981241]

Thind KK, Yamawaki R, Phanwar I, Zhang G, Wen X, Buckmaster PS. Initial loss but later excess of GABAergic synapses with dentate granule cells in a rat model of temporal lobe epilepsy. The Journal of Comparative Neurology. 2010; 518:647–667. [PubMed: 20034063]

Thom M, Liagkouras I, Martinian L, Liu J, Catarino CB, Sisodiya SM. Variability of sclerosis along the longitudinal hippocampal axis in epilepsy: A post mortem study. Epilepsy Research. 2012; 102:45–59. [PubMed: 22608064]

Tóth K, Eröss L, Vajda J, Halász P, Freund T, Maglóczky Z. Loss and reorganization of calretinin-containing interneurons in the epileptic human hippocampus. Brain. 2010; 133:2763–2777. [PubMed: 20576695]

Toyoda I, Bower MR, Leyva F, Buckmaster PS. Early activation of ventral hippocampus and subiculum during spontaneous seizures in a rat model of temporal lobe epilepsy. The Journal of Neuroscience. 2013; 33:11100–11115. [PubMed: 23825415]

Van Paesschen W, Revesz T, Duncan JS, King MD, Connelly A. Quantitative neuropathology and quantitative magnetic resonance imaging of the hippocampus in temporal lobe epilepsy. Annals of Neurology. 1997; 42:756–766. [PubMed: 9392575]

Waldau B, Hattiangady B, Kuruba R, Shetty AK. Medial ganglionic eminence-derived neural stem cell grafts ease spontaneous seizures and restore GDNF expression in a rat model of chronic temporal lobe epilepsy. Stem Cells. 2010; 28:1153–1164. [PubMed: 20506409]

Wei D, Yang F, Wang Y, Yang F, Wu C, Wu SX, Jiang W. Degeneration and regeneration of GABAergic interneurons in the dentate gyrus of adult mice in experimental models of epilepsy. CNS Neuroscience & Therapeutics. 2015; 21:52–60. [PubMed: 25272022]

West MJ, Slomianka L, Gundersen HJ. Unbiased stereological estimation of the total number of neurons in the subdivisions of the rat hippocampus using the optical fractionator. Anatomical Record. 1991; 231:482–497. [PubMed: 1793176]

Wetherington J, Serrano G, Dingledine R. Astrocytes in the epileptic brain. Neuron. 2008; 58:168–178. [PubMed: 18439402]

Williamson A, Patrylo PR, Spencer DD. Decrease in inhibition in dentate granule cells from patients with medial temporal lobe epilepsy. Annals of Neurology. 1999; 45:92–99. [PubMed: 9894882]

Wittner L, Maglóczky Z, Borhegyi Z, Halász P, Toth S, Eröss L, … Freund TF. Preservation of perisomatic inhibitory input of granule cells in the epileptic human dentate gyrus. Neuroscience. 2001; 108:587–600. [PubMed: 11738496]

Yu J, Swietek B, Proddutur A, Santhakumar V. Dentate total molecular layer interneurons mediate cannabinoid-sensitive inhibition. Hippocampus. 2015; 25:884–889. [PubMed: 25603947]

Zhang W, Thamattoor AK, LeRoy C, Buckmaster PS. Surviving mossy cells enlarge and receive more excitatory synaptic input in a mouse model of temporal lobe epilepsy. Hippocampus. 2015; 25:594–604. [PubMed: 25488607]

Zhang W, Yamawaki R, Wen X, Uhl J, Diaz J, Prince DA, Buckmaster PS. Surviving hilar somatostatin interneurons enlarge, sprout axons, and form new synapses with granule cells in a mouse model of temporal lobe epilepsy. The Journal of Neuroscience. 2009; 29:14247–14256. [PubMed: 19906972]

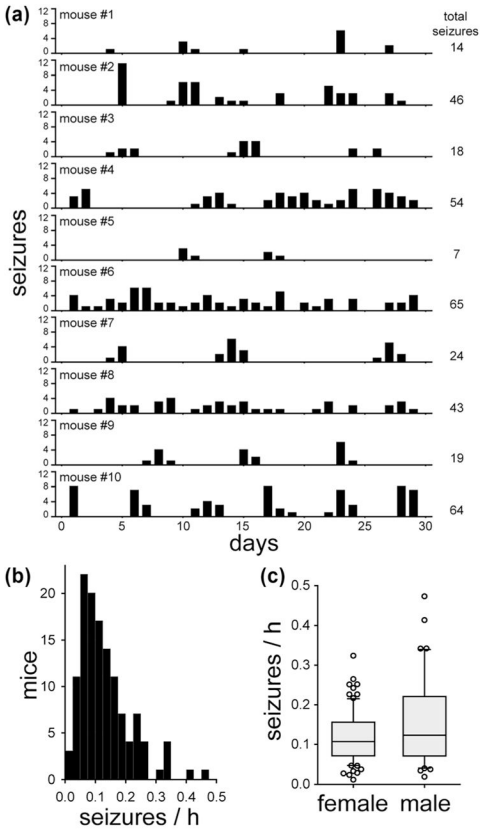

FIGURE 1.

Frequency of spontaneous, behavioral seizures in epileptic pilocarpine-treated mice. (a) Example of data from 10 mice. Mice were video-recorded 9 hr/day, every day for 1 month. Seizures of grade 3 or greater on the Racine (1972) scale were counted. (b) Histogram showing the distribution of seizure frequency for all the mice in this study. (c) Seizure frequency was not significantly different in female ($n = 82$) and male mice ($n = 45$, $p = 0.327$, Mann–Whitney rank sum test). In the box plots, the boundary of the box closest to zero indicates the 25th percentile, a line within the box marks the median, and the boundary of the box farthest from zero indicates the 75th percentile. Whiskers (error bars) above and below the box indicate the 90th and 10th percentiles. Markers indicate data points outside the 90th and 10th percentiles

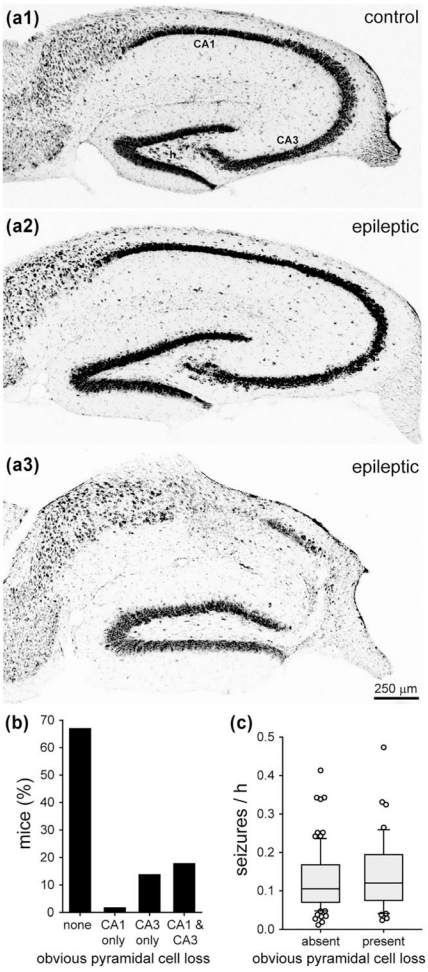

FIGURE 2.

No significant effect of obvious pyramidal cell loss on seizure frequency in epileptic pilocarpine-treated mice. Nissl staining of the hippocampus in a control mouse (a1), an epileptic mouse with obvious hilar neuron loss (a2), and an epileptic mouse with obvious loss of neurons in the hilus, CA1, and CA3 (a3). h = hilus. (b) Percentage of epileptic pilocarpine-treated mice with and without obvious pyramidal cell loss. (c) No significant difference in seizure frequency of mice with and without obvious pyramidal cell loss (p = 0.426, Mann–Whitney rank sum test)

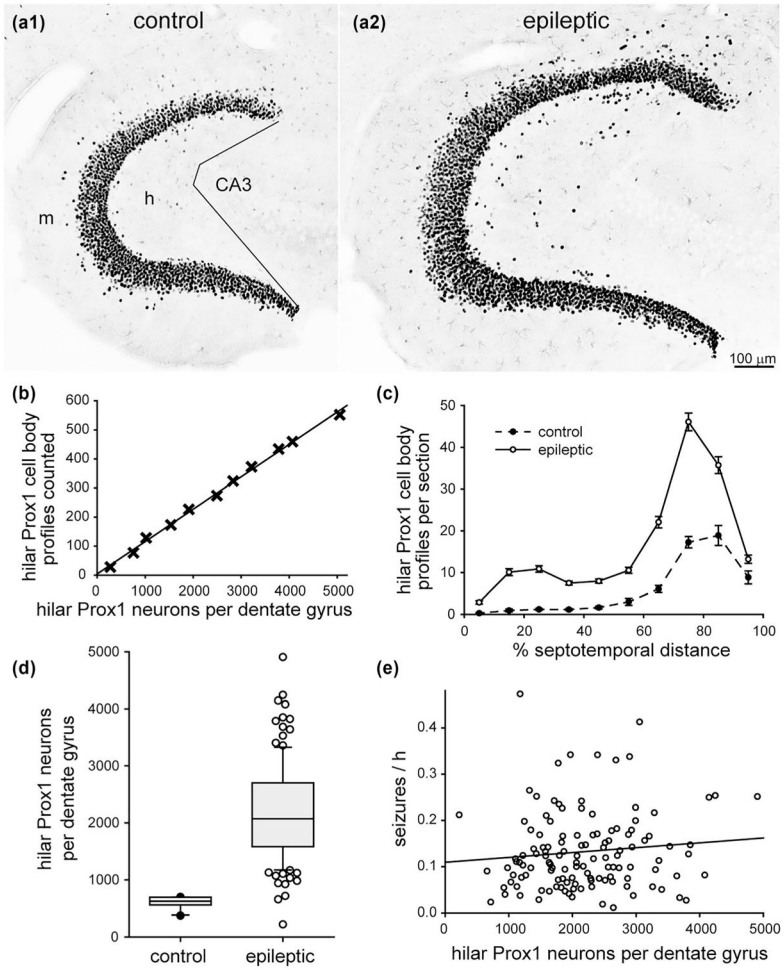

FIGURE 3.

No significant correlation between the number of hilar ectopic granule cells and seizure frequency in epileptic pilocarpine-treated mice. Prox1-immunostaining of the dentate gyrus in a control (a1) and epileptic mouse (a2). The dentate gyrus is larger and contains more Prox1-positive neurons in the granule cell layer and hilus of the epileptic mouse. Sections are 70% of the distance from the septal pole to the temporal pole of the hippocampus. Lines in (a1) indicate the border between the hilus (h) and CA3 field. g = granule cell layer; m = molecular layer. (b) High correlation between the number of hilar Prox1-positive cell body profiles counted and the number of hilar Prox1-positive neurons per dentate gyrus estimated by the optical fractionator method in a subset of mice from this study ($R = 0.998$, $p < 0.001$, ANOVA). (c) Septotemporal distribution of hilar Prox1-positive cell body profiles per section. Values represent mean ± *SEM*. (d) More hilar Prox1-positive neurons per dentate gyrus in epileptic mice ($n = 126$) compared to controls ($n = 10$, $p < 0.001$, Mann–Whitney rank sum test). (e) No significant correlation between the number of hilar Prox1-positive neurons per dentate gyrus and seizure frequency ($R = 0.0763$, $p = 0.398$, ANOVA)

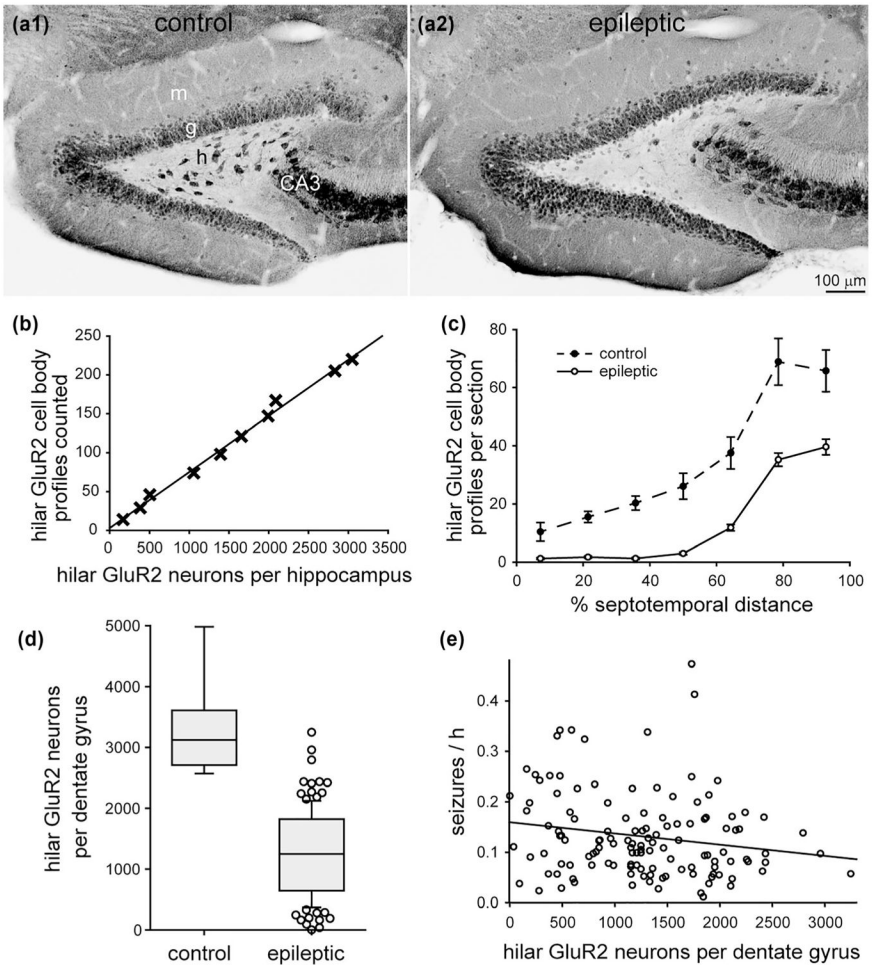

FIGURE 4.

No significant correlation between the number of mossy cells and seizure frequency in epileptic pilocarpine-treated mice. GluR2-immunostaining of the dentate gyrus from a control (a1) and epileptic mouse (a2). Sections are 50% of the distance from the septal pole to the temporal pole of the hippocampus. g = granule cell layer; h = hilus; m = molecular layer. (b) High correlation between the number of hilar GluR2-positive cell body profiles counted and the number of hilar GluR2-positive neurons per dentate gyrus estimated by the optical fractionator method in a subset of mice from this study ($R = 0.997$, $p < 0.001$, ANOVA). Only hilar GluR2-positive cells with a soma diameter >12 µm were counted. (c) Septotemporal distribution of hilar GluR2-positive cell bodies. Values represent mean ± *SEM*. (d) Fewer hilar GluR2-positive neurons in epileptic mice ($n = 127$) compared to controls ($n = 9$, $p \leq 0.001$, Mann–Whitney rank sum test). (e) No significant correlation between the number of hilar GluR2-positive neurons per dentate gyrus and seizure frequency ($R = 0.156$, $p = 0.079$, ANOVA)

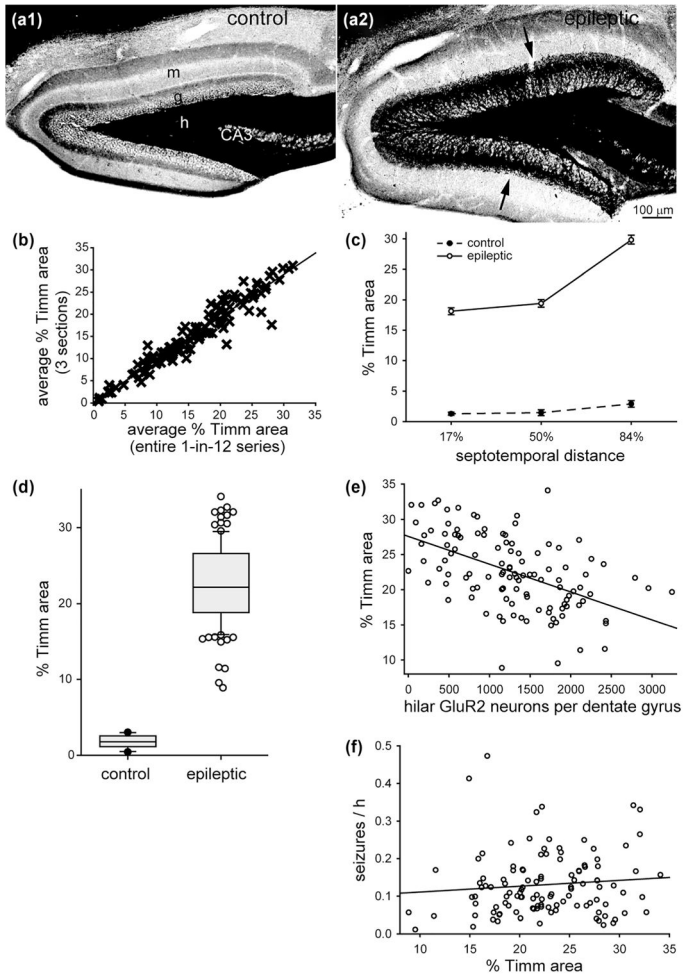

FIGURE 5.

No significant correlation between mossy fiber sprouting and seizure frequency in epileptic pilocarpine-treated mice. Timm staining of the dentate gyrus from a control (a1) and epileptic mouse (a2). Sections are 50% of the distance from the septal pole to the temporal pole of the hippocampus. g = granule cell layer; h = hilus; m = molecular layer. Mossy fiber sprouting is evident as black Timm staining in the granule cell layer and inner molecular layer in the epileptic mouse (arrows). (b) High correlation (slope = 1.049, $R = 0.961$, $p < 0.001$, Spearman rank order correlation) between the percent area of the granule cell layer plus molecular layer with black Timm staining measured two ways: (1) as the average of three sections (17, 50, and 84% of the distance from the septal pole to the temporal pole) and (2) as the average of the entire 1-in-12 series of sections. Data from Buckmaster and Lew (2011), Lew and Buckmaster (2011), and Heng et al. (2013). (c) Septotemporal distribution of percent Timm-positive area. Values represent mean ± *SEM*. (d) Larger percent Timm-positive area in epileptic pilocarpine-treated mice ($n = 114$) compared to controls ($n = 10$, $p \leq 0.001$, Mann–Whitney rank sum test). (e) Significant negative correlation between percent Timm-positive area and number of large (>12 μm soma diameter) hilar GluR2-positive neurons per dentate gyrus ($R = 0.515$, $p < 0.001$, ANOVA). (f) No significant correlation between percent Timm-positive area and seizure frequency ($R = 0.178$, $p = 0.058$, ANOVA)

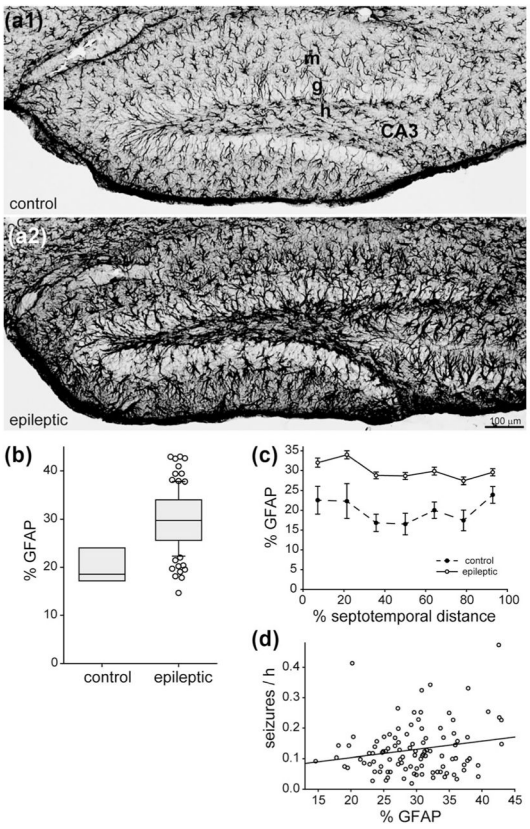

FIGURE 6.

No significant correlation between astrogliosis and seizure frequency in epileptic pilocarpine-treated mice. GFAP-immunostaining of the dentate gyrus in a control (a1) and epileptic mouse (a2). The dentate gyrus is larger and GFAP-immunoreactivity is increased in the epileptic mouse. Sections are 38% of the distance from the septal pole to the temporal pole of the hippocampus. g = granule cell layer; h = hilus; m = molecular layer. (b) The percent area of the dentate gyrus that was GFAP-positive was larger in epileptic mice (n = 103) compared to controls (n = 7, p <0.001, t test). (c) Septotemporal distribution of percent area that was GFAP-positive. Values represent mean ± *SEM*. (d) No significant correlation between percent area that was GFAP-positive and seizure frequency (R = 0.116, p = 0.244, Spearman rank order correlation)

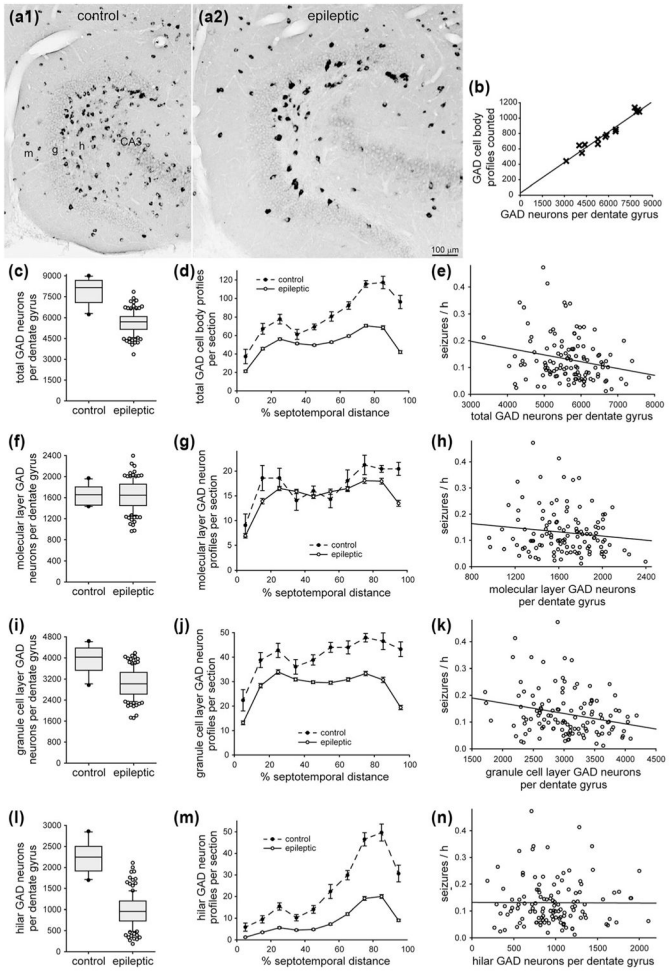

FIGURE 7.

Significant negative correlation between the number of GABAergic neurons in the dentate gyrus and seizure frequency in epileptic pilocarpine-treated mice. GAD in situ hybridization in sections of the dentate gyrus in a control (a1) and epileptic mouse (a2). The dentate gyrus is larger in the epileptic mouse. There are fewer GAD-positive neurons, but they are labeled more intensely in the epileptic mouse. Sections are 75% of the distance from the septal pole to the temporal pole of the hippocampus. g = granule cell layer; h = hilus; m = molecular layer. (b) High correlation between the number of hilar GAD-positive cell body profiles counted and the number of GAD-positive neurons per dentate gyrus estimated by the optical fractionator method in a subset of mice in this study ($R = 0.977$, $p < 0.001$, ANOVA). (c) Fewer total GAD-positive neurons per dentate gyrus in epileptic mice ($n = 122$) compared to controls ($n = 10$, $p < 0.001$, t test). (d) Septotemporal distribution of GAD-positive cell body profiles per section. Values represent mean ± *SEM*. (e) Significant negative correlation between the total number of GAD-positive neurons per dentate gyrus and seizure frequency ($R = 0.199$, $p = 0.029$, ANOVA). (f) No significant difference in the number of GAD-positive neurons in the molecular layer per dentate gyrus in epileptic mice compared to controls ($p = 0.999$, t test). (g) Septotemporal distribution of molecular layer GAD-positive cell body profiles per section. (h) No significant correlation between the total number of

molecular layer GAD-positive neurons per dentate gyrus and seizure frequency ($R = 0.129$, $p = 0.160$, ANOVA). (i) Fewer GAD-positive neurons in the granule cell layer per dentate gyrus in epileptic mice compared to controls ($p < 0.001$, *t* test). (j) Septotemporal distribution of granule cell layer GAD-positive cell body profiles per section. (k) Significant negative correlation between the number of granule cell layer GAD-positive neurons per dentate gyrus and seizure frequency ($R = 0.229$, $p = 0.012$, ANOVA). (l) Fewer GAD-positive neurons in the hilus per dentate gyrus in epileptic mice compared to controls ($p < 0.001$, Mann–Whitney rank sum test). (m) Septotemporal distribution of hilar GAD-positive cell body profiles per section. (n) No significant correlation between the number of hilar GAD-positive neurons per dentate gyrus and seizure frequency ($R = 0.001$, $p = 0.996$, ANOVA)

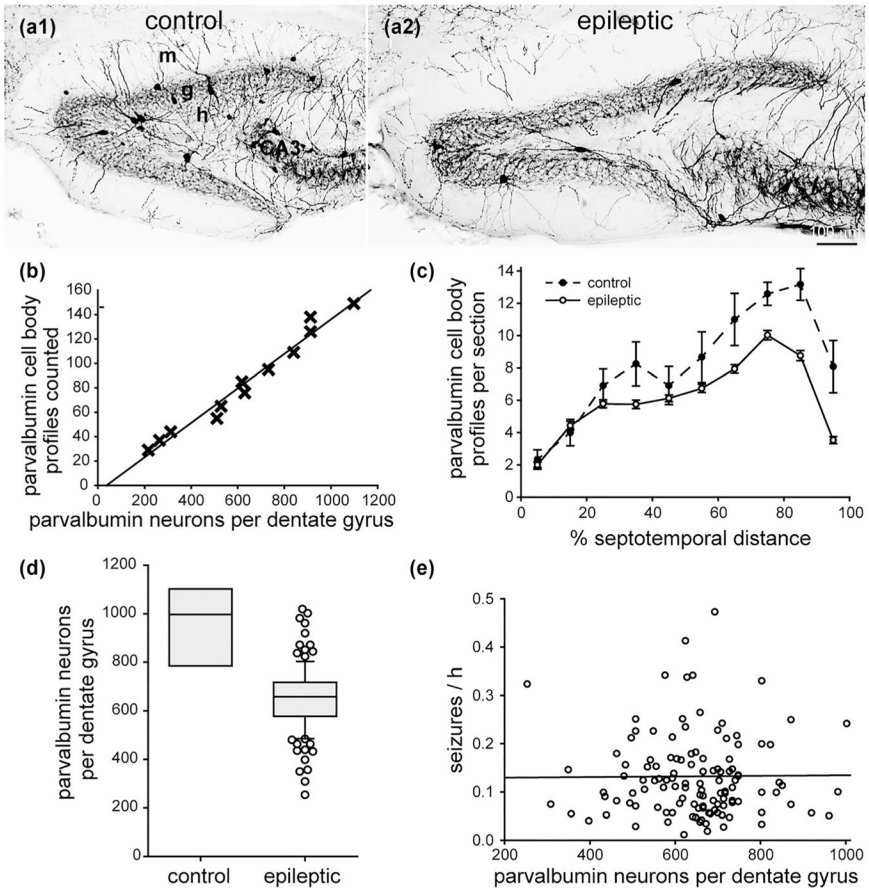

FIGURE 8.

No significant correlation between the number of parvalbumin-positive interneurons in the dentate gyrus and seizure frequency in epileptic pilocarpine-treated mice. Parvalbumin-immunostaining of the dentate gyrus in a control (a1) and epileptic mouse (a2). The dentate gyrus is larger but contains fewer parvalbumin-positive neurons in the epileptic mouse. Sections are 45% of the distance from the septal pole to the temporal pole of the hippocampus. g = granule cell layer; h = hilus; m = molecular layer. (b) High correlation between the number of parvalbumin-positive cell body profiles counted and the number of parvalbumin-positive neurons per dentate gyrus estimated by the optical fractionator method in a subset of mice from this study ($R = 0.985$, $p < 0.001$, ANOVA). (c) Septotemporal distribution of parvalbumin-positive cell body profiles per section. Values represent mean ± *SEM*. (d) Fewer parvalbumin-positive neurons per dentate gyrus in epileptic mice ($n = 122$) compared to controls ($n = 8$, $p < 0.001$, *t* test). (e) No significant correlation between the number of parvalbumin-positive neurons per dentate gyrus and seizure frequency ($R = 0.002$, $p = 0.979$, ANOVA)

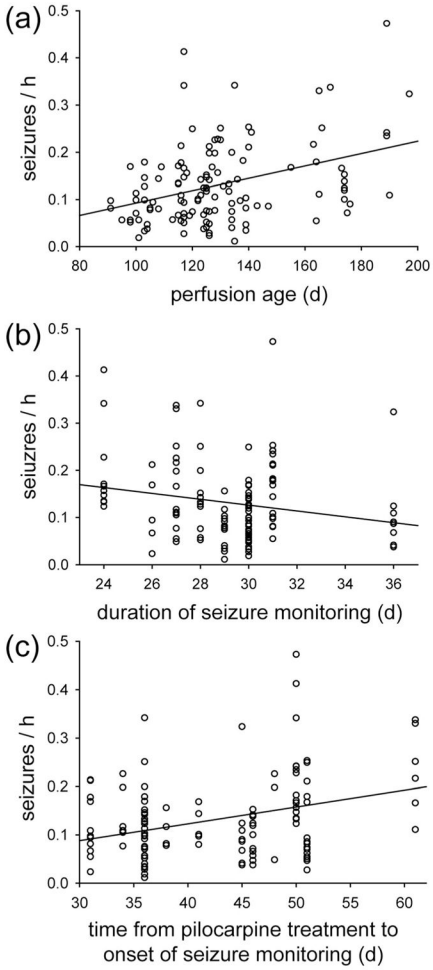

FIGURE 9.

Significant correlation between perfusion age and seizure frequency in epileptic pilocarpine-treated mice ($R = 0.302$, $p < 0.001$, ANOVA) (a). (b) No significant correlation between duration of seizure monitoring and seizure frequency ($R = -0.169$, $p = 0.061$, Spearman rank order correlation). (c) Significant correlation between seizure frequency and time from pilocarpine treatment to seizure monitoring ($R = 0.274$, $p = 0.002$, ANOVA)

TABLE 1

Anatomical sampling parameters

	Prox1	GluR2	GAD	parvalbumin
Neuron profile counting				
Section sampling	1-in-12	1-in-24	1-in-12	1-in-12
Sections/mouse[a]	14.7	7.4	14.7	14.7
Profiles[b]/mouse[a]	251	94	808	84
Optical fractionator counting				
Mice	11	10	14	12
Section sampling	1-in-12	1-in-24	1-in-12	1-in-12
Area sampling	Entire hilus, except within 25 μm of granule cell layer	Entire hilus	Dentate gyrus, 80 × 80 μm counting grid, 50 × 50 μm counting frame	Entire dentate gyrus
Caps[c]/mouse[a]	205	63	206	52
Profiles-to-neurons correlation coefficient	0.998	0.997	0.977	0.985

[a] Values represent averages.

[b] Cell profiles were counted with a 20× objective. Profiles were counted even if they were cut at the surface of the section.

[c] Cell caps were counted with a 100× objective. Caps were counted only if they were not cut at the surface of the section.

TABLE 2

Primary antibodies

Antigen	Host	Dilution	Immunogen	Source	Catalog #	RRID
Prox1	Rabbit, polyclonal	1:40,000	C-terminal 15 amino acids of mouse Prox1	Covance	PRB-238C	AB_10064230
Parvalbumin	Rabbit, polyclonal	1:100,000	Rat muscle parvalbumin	Swant	PV 25	AB_10000344
GluR2	Rabbit, polyclonal	0.5 μg/ml	Synthetic peptide from rat GluR2 conjugated to BSA	Millipore	AB1768	AB_2247874
GFAP	Rabbit, polyclonal	1:64,000	Cow spinal cord GFAP	Dako	Z0334	AB_10013382